Weak, Seismogenic Faults Inherited From Mesozoic Rifts Control Mountain Building in the Andean Foreland

Sam Wimpenny[1] 📛

[1]COMET, Bullard Laboratories, Department of Earth Sciences, University of Cambridge, Cambridge, UK

Abstract New earthquake focal mechanism and centroid depth estimates show that the deformation style in the forelands of the Andes is spatially correlated with rift systems that stretched the South American lithosphere in the Mesozoic. Where the rifts trend sub-parallel to the Andean range front, normal faults inherited from the rifts are being reactivated as reverse faults, causing the 30–45 km thick seismogenic layer to break up. Where the rift systems are absent from beneath the range front, the seismogenic layer is bending and being thrust beneath the Andes like a rigid plate. Force-balance calculations show that the faults inerhited from former rift zones have an effective coefficient of static friction $\mu' < 0.2$. In order for these frictionally weak faults to remain seismogenic in the lower crust, their wall rocks are likely to be formed of dry granulite. Xenolith data support this view, and suggest that parts of the lower crust are now mostly metastable, having experienced temperatures at least $75–250°C$ hotter than present. The conditions in the lower crust make it unlikely that highly pressurized free water, or networks of intrinsically weak phyllosilicate minerals, are the cause of their low effective friction, as, at such high temperatures, both mechanisms would cause the faults to deform through viscous creep and not frictional slip. Therefore pre-existing faults in the Andean forelands have remained weak and seismogenic after reactivation, and have influenced the style of mountain building in South America. However, the controls on their mechanical properties in the lower crust remain unclear.

Plain Language Summary This study is concerned with the controls on how mountain ranges grow. I show that the locations and types of earthquakes along the margins of the Andes mountains, which are generated when the mountain range grows, vary systematically with the positions of ancient fault zones. Where ancient faults lie along the margins of the Andes the entire crust is breaking up through slip on these faults. Where the same faults are not present along the margins of the Andes, the crust is being pushed beneath the mountains like a rigid plate. Therefore, the strength of faults along the margins of the Andes play a critical role in the growth of the mountain range. Notably, the earthquake-generating faults along the margins of the Andes are much weaker than predicted by laboratory experiments, and the physical reason for their weakness remains unclear.

1. Introduction

The frictional properties of faults in the forelands of mountain ranges may play a key role in controlling the style and location of mountain building (Jackson, 2002a; Butler et al., 2006). Where faults are too strong to rupture in response to the forces acting through the lithosphere, the foreland may behave as a rigid plate and be thrust beneath the mountain range below a shallowly dipping décollement. In contrast, where faults are weak enough to rupture in response to the forces acting through the lithosphere, the foreland may break up, creating a region of distributed deformation and intense seismicity.

These contrasting styles of mountain building have been recognised along the eastern margin of the Andes in South America on the basis of outcrop patterns and fault spacing (Jordan et al., 1983; Kley et al., 1999; Ramos, 2010b), and the focal mechanisms and depth extent of seismicity (Suarez et al., 1983; Devlin et al., 2012). The along-strike changes in the foreland deformation style correlate with proxies for the integrated strength of the lithosphere such as the effective elastic thickness (Watts et al., 1995; Stewart & Watts, 1997), as well as the pattern and timing of Miocene uplift (Gubbels et al., 1993; Kennan et al., 1997) and rotations inferred from paleomagnetic declination anomalies (Lamb, 2000; Barke et al., 2007) within the adjacent high Andes. Therefore, the Andean forelands are a unique environment to study the frictional properties of faults and their influence on the growth of mountain ranges.

Our understanding of fault friction remains rooted in the results of laboratory experiments. Lab measurements of the static coefficient of friction (μ) for most rock types are consistently between 0.6 and 0.85, a widely applied result known as "Byerlee's Law" (Byerlee, 1978). However, *in-situ* estimates of the effective coefficient of static friction (μ') on seismogenic faults are between 0.05 and 0.3 (Copley, 2018). The differences between the laboratory and *in-situ* estimates of static friction have been accounted for by invoking either: (a) highly pressurized pore fluids, often assumed to be water, that reduce the effective stresses within the cores of active faults (Hubbert & Rubey, 1959), or (b) networks of intrinsically weak phyllosilicates produced through water-mediated alteration of the rocks in the cores of active faults (Imber et al., 1997). Geological evidence of both transiently high fluid pressures and phyllosilicate-rich lithologies is widespread within ancient continental fault zones exhumed from depths of less than 20 km, indicating that water-assisted processes may be critical to generating frictionally weak faults in the upper crust (Sibson, 1990; Collettini et al., 2019).

Despite the consensus regarding the geological controls on fault mechanics in the upper crust, the mechanics of seismogenic faults in the lower crust remain enigmatic. For example, along the margins of the Andes mountains in central Peru, seismogenic faults cutting through the ~40 km thick foreland crust have been shown to have a low effective coefficient of friction compared to Byerlee's Law (Wimpenny et al., 2018). Unlike most continental fault zones, which only generate earthquakes in the upper 10–20 km of the crust, these faults in central Peru remain seismogenic into the lower crust. For faults to remain seismogenic at such high pressures and temperatures, the lower crust that surrounds them is thought to be formed of a load-bearing network of anhydrous minerals that contains little or no free pore water (Yardley & Valley, 1997; Jackson et al., 2004). As a result, there is reason to question whether the same water-assisted mechanisms that have been invoked to account for weak faults in the upper crust are also applicable to these seismogenic, lower-crustal fault zones. Vast areas of anhydrous rocks regularly form the forelands of the highest mountain ranges on Earth (Jackson et al., 2021; Weller et al., 2021). Therefore, developing an understanding of the mechanics of fault zones within the anhydrous lower crust, like those in central Peru, is important for understanding the style of deformation along the margins of active and ancient mountain ranges.

In this study, I determine the mechanical properties and Mesozoic-Cenozoic history of the active fault zones along the eastern margins of the Andes, and explore how these faults influence the distribution and style of mountain building. I begin by using new estimates of the focal mechanisms and centroid depths of earthquakes to map out variations in the style of crustal deformation throughout the Andean forelands. I then compare the pattern of seismicity with the location of pre-existing faults in the South American foreland lithosphere. I place bounds on the frictional properties of the seismogenic faults within the Andean forelands using force-balance calculations, and use published xenolith thermobarometry and thermo-kinematic modeling to constrain the geological conditions in the lower crust through which the seismogenic faults cut. Finally, I discuss the implications of these findings for structural inheritance and growth of mountain ranges, and the mechanisms that may account for the frictional properties of faults within the anhydrous lower crust.

2. Seismicity in the Forelands of the Andes

To determine the focal mechanisms and centroid depths of moderate-magnitude earthquakes in the Andean forelands, I used waveform modeling of teleseismic *P* and *SH* waves and their depth phases (*pP*, *sP* and *sS*). For earthquakes of $M_w \gtrsim 5.4$, I fit the shape and amplitude of the long-period (15–100 s) teleseismic *P* and *SH* waves using the body-waveform inversion algorithm of Zwick et al. (1994). This method has been used extensively in the region (for example, Devlin et al., 2012) and yields earthquake centroid depth estimates with uncertainties of $\pm$2–5 km. For earthquakes of $4.8 < M_w < 5.4$ typically only the *P* waves, and the *pP* and *sP* depth phases, are clear on teleseismic seismograms. I calculated the depths of these smaller-magnitude earthquakes by fitting synthetic waveforms to either broadband vertical-component seismograms, or to a stack of short-period vertical-component seismograms recorded at small-aperture seismic arrays (for example, Craig et al., 2012). This method can typically constrain the centroid depth to within $\pm$1–3 km. All of these methods have been described extensively in the literature (Molnar & Lyon-Caen, 1989; Taymaz et al., 1990; Craig et al., 2011), therefore further details regarding the data processing, inversion strategy, the velocity structure used and the modeling uncertainties are provided in Text S1 in Supporting Information S1.
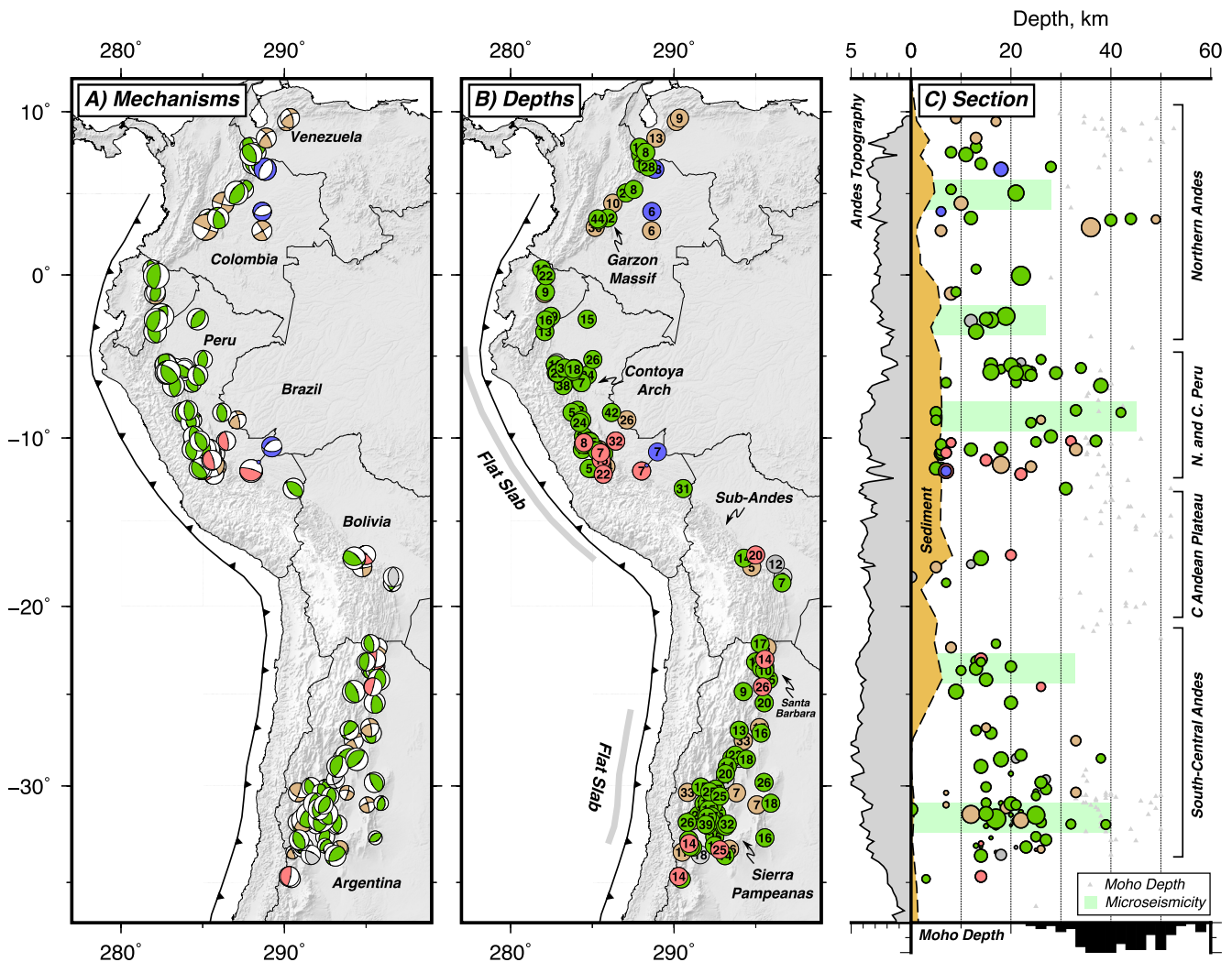
Figure 1. Well-constrained focal mechanisms and centroid depths for earthquakes in the forelands of the Andes. (a) Earthquake mechanisms colored by the mechanism type, with reverse faults in green, low-angle thrusts in red, normal faults in blue and strike-slip faults in brown. (b) Earthquake centroid depths in kilometres. (c) Section of the centroid depth distribution in the forelands along-strike. Gray circles in (c) are events that do not have a well-constrained focal mechanism. Each circle is scaled in size by the earthquake magnitude. Green bars represent the depth extent of microseismicity from local earthquake and aftershock surveys. The Moho depth variation in the foreland is shown by gray triangles and is taken from receiver function studies (Assumpção et al., 2013; Poveda et al., 2015; Condori et al., 2017). The sediment thickness in the foreland is taken from Golonka et al. (1995).

In addition to my own modeling of 45 new earthquakes (see Table 1 and Figures 4–50 in Supporting Information S1), I compiled 108 earthquake focal mechanisms and centroid depths derived using similar methods from the literature (Suarez et al., 1983; Chinn & Isacks, 1983; Kadinsky-Cade et al., 1985; Assumpção & Suarez, 1988; Assumpção & Araujo, 1993; Alvarado et al., 2005; Alvarado & Beck, 2006; Meigs & Nabelek, 2010; Devlin et al., 2012; Wimpenny et al., 2018). Microseismicity located using local seismometer networks provide additional constraints on the depth extent of seismicity within the forelands (Smalley & Isacks, 1990; Smalley et al., 1993; Cahill et al., 1992; Dorbath et al., 1986; Legrand et al., 2005; Dimate et al., 2003; Richardson et al., 2012; Vaca et al., 2019; Rivas et al., 2019). The resulting compilation of earthquakes is shown in Figure 1 along with the distribution of the Moho depth in the forelands, which varies between 35 and 48 km (Assumpção et al., 2013; Poveda et al., 2015; Condori et al., 2017). I describe the along-strike variation in the earthquake focal mechanisms and centroid depths below.

Throughout the northern Andes of Venezuela, Colombia and Ecuador, ~N-S to ~NE-SW striking reverse and strike-slip faulting is mostly concentrated along the range front and extends from 5 to 49 km depth. Aftershocks recorded by temporary seismometer deployments in Colombia (Dimate et al., 2003) and Ecuador (Legrand

et al., 2005) following M_w six earthquakes located microseismicity down to 30 km. Seismicity deeper than 30 km is only found in a cluster of four earthquakes with centroid depths between 34 and 49 km depth that ruptured faults within the Garzon Massif of south-central Colombia (Figures 1b and 1c). These four earthquakes do not appear to be representative of the depth extent of seismicity along the whole northern Andes, as elsewhere both moderate-magnitude earthquakes and microseismicity are consistently confined to depths of less than 30 km.

Earthquakes east of the range front in Colombia have shallow (<20 km) normal-faulting mechanisms, indicating that the top of the foreland crust is in extension. These normal-faulting earthquakes have previously been interpreted to reflect the bending of the foreland lithosphere under the weight of the Andes (Wimpenny et al., 2018). At a similar distance east of the range front of the Ecuadorian Andes, the shallow crust at 15 km depth is in compression. Therefore the stress state within the top 20 km of the foreland crust varies perpendicular to the strike of the mountain range, as well as along strike.

In northern and central Peru, the forelands are characterized by reverse-faulting earthquakes that extend throughout the crust from 5 to 42 km depth. The same depth distribution of earthquakes has also been observed by a temporary seismometer deployment that recorded microseismicity down to 45 km depth beneath the forelands of central Peru (Dorbath et al., 1986; Suárez et al., 1990). Although the majority of the earthquakes are concentrated beneath the steep topography along the eastern margin of the Andes, a significant number lie well into the foreland forming a ~300 km-wide zone of distributed compressional deformation. This zone of distributed deformation coincides with crystalline basement highs that have been uplifted relative to the foreland basin sediments during the Neogene (e.g., the Contoya Arch; see Kley et al. (1999)).

There have been few earthquakes in the sub-Andean fold-thrust belt that wraps around the margins of the central Andean plateau in southern Peru and Bolivia. The largest earthquakes accommodate low-angle thrust faulting at depths ≤20 km, whilst the lower 10–20 km of the foreland crust has experienced only one moderate-magnitude earthquake in the last 50 years — a reverse-faulting earthquake at 31 km depth. A 7 km deep, normal-faulting earthquake east of the range front in southern Peru indicates that the shallow part of the foreland crust is in extension. Geodetic, seismological and structural observations suggest that the foreland crystalline basement is underthrusting the central Andean plateau along a shallowly dipping décollement in this region (Lyon-Caen et al., 1985; Allmendinger & Gubbels, 1996; Brooks et al., 2011; Weiss et al., 2015).

A sharp transition in the foreland seismicity occurs across the Bolivia-Argentina border. At latitude 23°S, the foreland transitions from being predominantly aseismic within the Bolivian sub-Andes to the north, to experiencing frequent ~N-S striking reverse- and low-angle thrust-faulting earthquakes in the Santa Barbara Ranges to the south. Across the same section of foreland, the trains of closely spaced anticlines that characterize the surface morphology in the Bolivian sub-Andes abruptly stop, and the foreland structures transition southwards into widely spaced, east and west-verging reverse faults in the Santa Barbara Ranges (Kley & Monaldi, 2002). Microseismicity and moderate-magnitude earthquakes beneath Santa Barbara have been recorded down to 35 km depth (Cahill et al., 1992).

South of latitude 26°S, the seismicity becomes more spatially distributed over an area that stretches 300–400 km from the margins of the Andes into the foreland, coincident with the basement uplifts of the Sierra Pampeanas (Jordan et al., 1983). The focal mechanisms indicate that the earthquakes are predominantly on ~N-S striking reverse-faults, with a component of strike-slip faulting on ~N–S or ~E–W striking planes. Most of the moderate-magnitude seismicity and microseismicity is concentrated between 10 and 30 km depth, but seismicity does extend to a maximum of 40 km depth beneath the forelands (Smalley & Isacks, 1990; Smalley et al., 1993).

The along-strike variability in the depth distribution of seismicity within the Andean forelands is consistently mirrored by the microseismicity recorded by local seismometer networks, indicating that the variations are real and are not related to limited sampling of infrequent moderate-magnitude earthquakes (Figure 2). The centroid depth distributions show a single peak within the mid-crust (Chinn & Isacks, 1983), and all of the seismicity is contained within a single layer that is similar in thickness to the crust (Figure 2). These observations are consistent with faults supporting the forces acting through the foreland lithosphere via resistance to slip in a seismogenic layer, which varies from 30 km thick in the northern Andes to 40–45 km thick in the central Peru and the south-central Andes. The seismogenic layer is underlain by a mostly aseismic mantle lithosphere (Maggi, Jackson, Priestley, & Baker, 2000). In addition to the along-strike variability in the thickness of the seismogenic
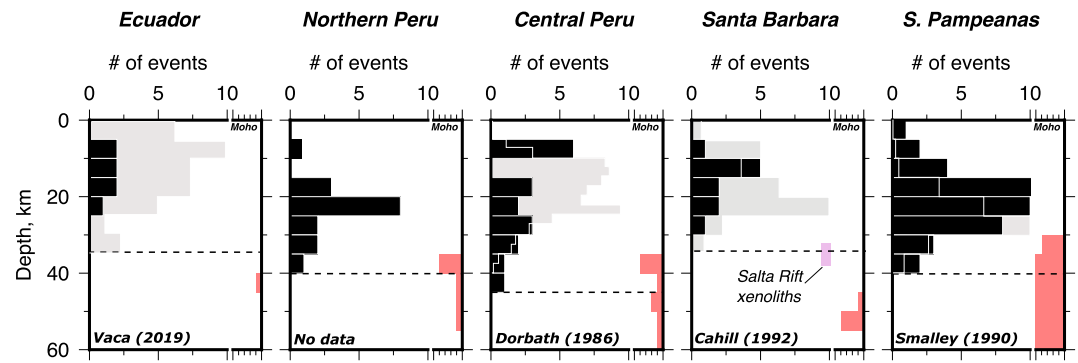
Figure 2. Histograms of the centroid depths of moderate-magnitude earthquakes (black bars), and regional and local microseismicity studies (gray bars with white outline), in different sections of the forelands. The maximum number of microseismic events in each region is normalised to 10 to display the relative distribution with depth. The source of the microseismicity data is shown in the bottom left of each plot. A histogram of the Moho depth in each region is also shown by the red bars on the right of each plot. The horizontal black-dashed line marks the thickness of the seismogenic layer T_s to the nearest 5 km. The depth range of granulite xenoliths erupted from the Salta Rift (discussed in Section 5) are shown by a purple bar.

layer within the forelands (Figure 1c), there is clear map-view variability in the frequency and spatial distribution of moderate-magnitude earthquakes. I explore the controls on these patterns further in the next section.

3. Relationship Between Seismicity and Foreland Structure

3.1. Flat Slabs

The structure of the subducting Nazca Plate has been inferred to correlate with the pattern of seismicity within the Andean forelands. Jordan et al. (1983) showed that, where the Nazca Plate subducts sub-horizontally beneath the Andes in northern Argentina (see regions marked "flat slab" on Figure 1b), the adjacent forelands are characterized by frequent compressional earthquakes that extend throughout the crust. In contrast, where the Nazca Plate dips steeply, such as around the central Andean plateau, the forelands experience less frequent seismicity that is mostly confined to the upper crust (see also Gutscher et al., 2000). The physical explanation for these trends was that the flat slab can cool the overriding lithosphere and increase the horizontal force transmitted between the subducting and overriding plates, causing the whole foreland crust in areas of flat-slab subduction to break up in compressional earthquakes.

The general patterns within the south-central Andes described by Jordan et al. (1983) and Gutscher et al. (2000) are also seen in the updated earthquake catalog presented in Figure 1. Foreland seismicity above the flat slab in Argentina appears deeper and more frequent than in the region to the north in the Bolivia sub-Andes. However, the same patterns are less clear in the northern Andes. Within northern Ecuador and Colombia, where newer models of the Nazca Plate geometry show it dipping continuously into the mantle (Hayes et al., 2018), the forelands are also characterized by frequent compressional earthquakes throughout the entire crust to depths of 30–49 km, just as in the areas with a flat slab (Figure 1). The moment release from foreland seismicity is larger in Ecuador than any other part of the Andean forelands, demonstrating that the amount of seismogenic deformation in the forelands does not always peak in areas underlain by a flat slab (Table 1). In addition, the deepest earthquakes anywhere in the Andean foreland occur in southern Colombia (Figure 1) — a region with a steeply dipping slab. Therefore, when considering the pattern of seismicity along the

Table 1
Comparison of Geodetic and Seismic Deformation Rates in the Andean Forelands

Location	v_x [mm/yr]	W [km]	$\dot{\varepsilon}_{xx}^{g}$ [10^{-8} 1/yr]	T_s [km]	$\dot{\varepsilon}_{xx}^{q}$ [10^{-8} 1/yr]	$\dot{\varepsilon}_{xx}^{q}/\dot{\varepsilon}_{xx}^{g}$ [%]
Northern and South-Central Andes						
S. Pampeanas	6 ± 1	400 ± 50	1.6 ± 0.4	40	1.50	70–130
C. Peru	3 ± 1	350 ± 50	0.9 ± 0.4	45	0.50	40–100
N. Peru	3 ± 1	350 ± 50	0.9 ± 0.4	40	0.85	65–170
Ecuador	5 ± 1	300 ± 50	1.8 ± 0.8	30	2.70	170–270
Central Andean Plateau						
S. Bolivia	7 ± 1	200 ± 50	3.5 ± 1.2	40	0.02	0.4–0.8
S. Peru	4 ± 1	200 ± 50	2.0 ± 1.2	40	0.20	6–25

Note. v_x is the range-perpendicular shortening rate inferred from the GPS measurements of Kendrick et al. (2001), Nocquet et al. (2014) and Kendrick et al. (2006), and W is the width of the deforming zone measured perpendicular to the range front based on earthquakes and geomorphology. $\dot{\varepsilon}_{xx}^{g}$ is the average horizontal strain rate perpendicular to the range, and is equivalent to v_x/W. $\dot{\varepsilon}_{xx}^{q}$ is the range-perpendicular horizontal strain rate inferred from a summation of earthquake moment tensors using a shear modulus of 30 GPa and the seismogenic thickness T_s.
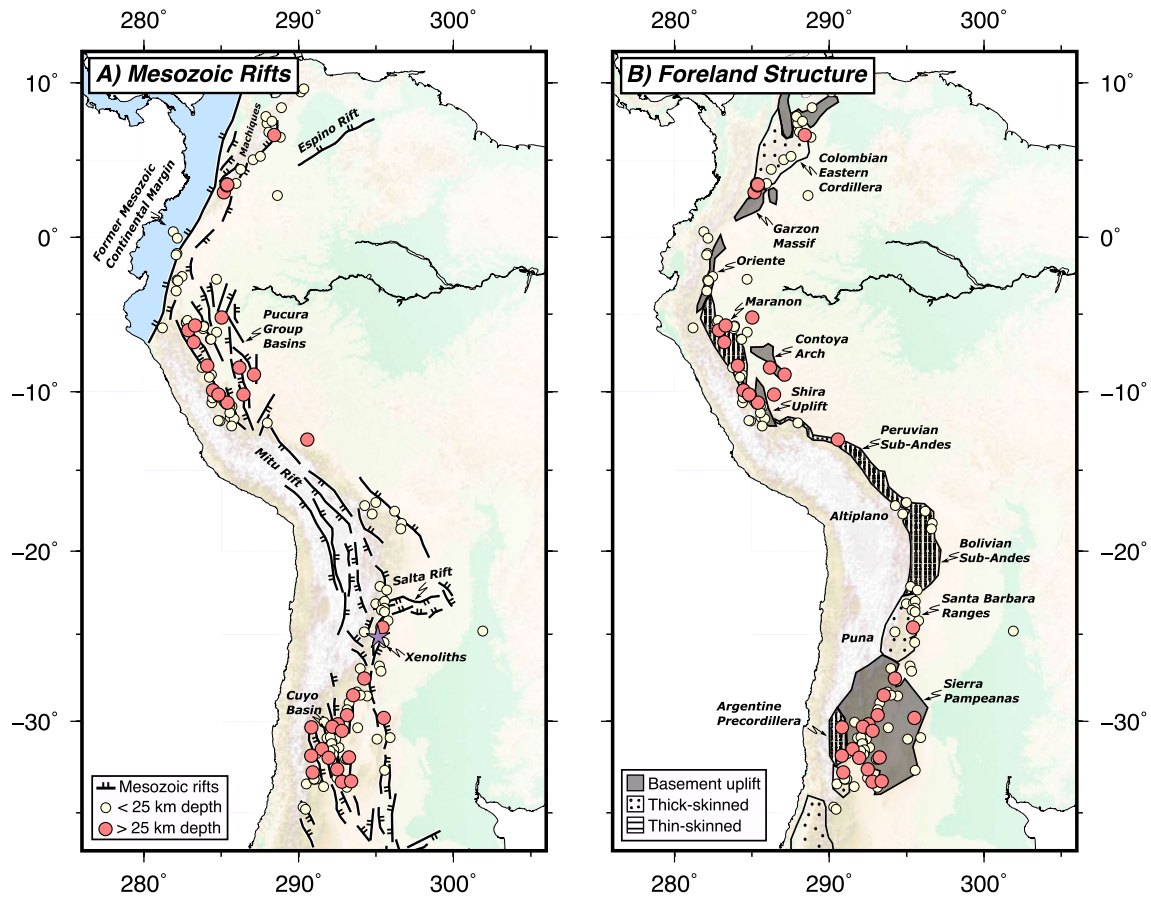
Figure 3. Earthquake distribution compared to the loci of Mesozoic rifts (a) and the structural style of deformation in the Andean forelands (b). The simplified traces of the Mesozoic rifts in (a) are taken from Ramos (2009) and McGroder et al. (2015). Earthquakes are shown by circles and are colored light red if they have a centroid depth >25 km. Rift-related faults running through the Chilean forearc and Andes are omitted to highlight regions where the rifts lie along the margins of the mountain range. The location of the xenolith suite of Lucassen et al. (1999) discussed in Section 5 is shown by a purple star. In (b) the along-strike variability in the structural style of foreland deformation is split into three different styles: thin-skinned, thick-skinned and basement uplifts. The deformation style is taken from Kley et al. (1999).

whole Andean chain, it appears that the shape of the Nazca Plate is not necessarily the controlling factor on the depth extent, moment release or mechanisms of the foreland earthquakes.

3.2. Inherited Structure

The influence of pre-Andean deformation structures, particularly those associated with Mesozoic rifting, on the location and style of active deformation is seen throughout the Andean forelands (for example, Coira et al., 1982; Kley et al., 2005; Mora et al., 2006; Charrier et al., 2015). These continental rifts were active between the late Permian and the Cretaceous, developed in response to the break up of Pangea (Ramos, 2010b; Spikings et al., 2016) and often follow boundaries inherited from earlier episodes of deformation (Ramos et al., 2002). Figure 3 shows the locations of the major Mesozoic rift-related faults mapped by Ramos (2009) and McGroder et al. (2015) based on seismic reflection data and geological outcrop, and their relationship with the foreland seismicity and the structural style of deformation.

Within northern and central Peru, and in the Sierra Pampeanas of Argentina, the Mesozoic rift systems form ~300 km wide belts of range-parallel faults that extend from the eastern margin of the high Andes into the foreland. In these regions, the forelands are associated with distributed upper- and lower-crustal compressional earthquakes that closely follows the map-view shape of the rift systems. At the surface the deformation is mostly characterized by "thick-skinned" structures, with crystalline basement being exhumed toward the surface along steeply dipping reverse faults (Kley et al., 1999; Ramos et al., 2002). In the Marañon Basin of northern Peru the rift systems trend beneath a superficial "thin-skinned" fold-thrust belt characterized by trains of anticlines formed

of sediments (Mathalone & Montoya, 1995; Hermoza et al., 2005), whilst the lower crust beneath the fold-thrust belt still remains highly seismogenic (Suarez et al., 1983).

In the northern Andes of Ecuador, Colombia and Venezuela, the Mesozoic rift systems trend through the mountain range and parallel to the eastern range front of the Andes, but do not extend more than ~50 km into the forelands. The distribution of seismicity mirrors this pattern, with reverse and strike-slip faulting earthquakes mostly clustering beneath the range front. In some cases, recent earthquakes beneath the range front can even be directly linked to inverted normal fault structures mapped at the surface or in seismic reflection profiles (Legrand et al., 2005; Mora et al., 2006).

Beneath the Santa Barbara Ranges of northern Argentina, the western branch of the Salta Rift consists of basins bound by ~N-S striking normal faults that trend beneath the Andean range front. The same region has experienced a number of moderate-magnitude earthquakes on ~N-S striking reverse faults and shows evidence for normal-fault reactivation in outcrop (Kley et al., 2005). However, in the eastern branch of the Salta Rift, where the rift-related faults strike ~E-W and are almost perpendicular to the range front, there have been no recent moderate-magnitude earthquakes. Therefore, the Mesozoic rifts appear to only be associated with moderate-magnitude earthquakes if the inherited normal faults and rift fabrics strike sub-parallel to the range front.

In contrast to the northern and south-central Andes, within southern Peru and Bolivia the Mesozoic rift systems trend through the interior of the central Andean plateau (for example, Sempere et al., 2002), and rifted basement is mostly absent beneath the range front (Figure 3a). Around the margins of the plateau, the thin-skinned sub-Andean fold-thrust belt has experienced far fewer earthquakes than the northern and southern Andean forelands, and the largest earthquakes are shallow, low-angle thrust faulting events. East of the range front, there have only been two earthquakes; the shallowest being a normal-faulting earthquake with a centroid depth of 7 km, and the deepest being a reverse-faulting earthquake with a centroid depth of 31 km. The same pattern of seismicity has been recognised in the Indian forelands south of Tibet (for example, Molnar et al., 1977), and is interpreted to reflect bending of the lithosphere in response to the vertical load of the mountain belt.

The remarkable spatial correlation between regions of frequent lower-crustal earthquakes, the Mesozoic rift systems, and the deformation style within the forelands suggests a physical link. The simplest explanation is that, along the margins of the northern and south-central Andes, range-parallel normal faults inherited from the Mesozoic rifts are being reactivated within the mid-lower crust as reverse faults, causing the whole seismogenic layer to break up in compression. A summation of the earthquake moment tensors in these regions using the method of Kostrov (1974) suggests that 40%–100% of the range-perpendicular shortening rates measured from GPS can be accounted for by seismogenic slip on faults (Table 1). In contrast, around the central Andean plateau the range-perpendicular shortening rates from recent seismicity are 0.5%–25% of the rates inferred from GPS (Table 1). Beneath the sub-Andes, the foreland is presumably too strong to deform significantly in response to the forces associated with mountain building. Therefore, instead of the foreland seismogenic layer breaking up in compression, it is bending and being thrust beneath the central Andean plateau as a relatively rigid plate (Watts et al., 1995). Shortening is instead accommodated by slip on a décollement that separates the rigid foreland from the overlying sub-Andean fold-thrust belt and by viscous shortening of the lower crust beneath the central Andean plateau (Allmendinger & Gubbels, 1996; Lamb, 2000; Brooks et al., 2011).

4. Strength of Inherited Faults in the Forelands

The pattern of seismicity in the forelands of the northern and south-central Andes demonstrates that faults inherited from Mesozoic rifts are breaking in reverse-faulting earthquakes, implying that the forces acting on these structures exceeds their frictional resistance to slip. In this section, I estimate the forces acting on these faults and place bounds on their frictional properties.

Gravity acting on differences in the thickness and density of the crust and mantle lithosphere between the Andes and its forelands generates a horizontal buoyancy force F_b that must be balanced by a horizontal force acting through the foreland lithosphere F_f, and resistance to deformation within the mountains (Dalmayrac & Molnar, 1981; Molnar & Lyon-Caen, 1988). It is likely that many parts of the Andes are close to the state of $F_b \approx F_f$ as the highest portions of the mountain range have relatively flat, plateau-like topography (Lamb, 2006). In addition, in the most rapidly deforming areas of the high Andes, such as the Cordillera Blanca in central Peru

Table 2
Parameter Range Used to Calculate the Buoyancy Force F_b at Different Points Along-Strike

Region	z_{lm} [km]	z_{lf} [km]	z_{cm} [km]	z_{cf} [km]	Δh [km]	F_b [TN/m]
Colombia	150–175	125–150	60–65	30–35	2.7–3.0	3.4 ± 0.4
Ecuador	100–150	125–150	50–60	30–35	2.8–3.0	3.2 ± 0.3
N. Peru	100–150	125–150	50–55	35–40	2.8–3.2	3.7 ± 0.4
C. Peru	100–150	125–175	65–75	35–40	3.8–4.2	5.4 ± 0.6
S. Peru	150–175	125–150	70–75	35–40	4.0–4.3	5.7 ± 0.6
Bolivia	150–200	125–150	70–75	35–40	3.5–3.8	5.1 ± 0.5
Puna	150–175	125–150	70–75	35–40	4.0–4.5	5.9 ± 0.7
Pampeanas	100–125	100–125	65–70	35–40	3.8–4.1	5.2 ± 0.4

Note. z_{lm} = lithosphere thickness beneath the mountains, z_{lf} = lithosphere thickness beneath the forelands, z_{cm} = crustal thickness beneath the mountains, z_{cf} = crustal thickness beneath the forelands, and Δh is the height difference between the mountain range and foreland. The mean of F_b and the 95th percentile range of models are quoted. The fixed parameters are: crustal density = 2,800 kg/m³, mantle density = 3,330 kg/m³, density difference between depleted mantle lithosphere and asthenosphere = −50 kg/m³, crustal thermal expansivity = 3×10^{-5} W/m/K, Moho temperature beneath the mountains 700–1000 °C, and Moho temperature beneath the forelands = 600–700 °C.

and in the Altiplano of southern Peru, seismicity rates and fault slip rates imply that deviations from $F_b = F_f$ are ≲0.5–0.7 × 10¹² N per meter along-strike, which is ≲10%–25% of F_b (Wimpenny et al., 2020). Therefore, to place a bound on the forces acting through the forelands F_f, I calculated the buoyancy forces F_b in eight different regions of the Andes using the method described in Copley and Woodcock (2016), with the range of parameters given in Table 2. The eight different regions were selected to encompass sections of the Andes where deformation within the mountains and forelands, and the height of the mountains, are relatively continuous along-strike.

Within Ecuador, Colombia and northern Peru, where the Andes are 2.8–3.5 km high, the calculated buoyancy forces are 3–4 × 10¹² N/m (Figure 4a). In Ecuador there is evidence for shortening within the high Andes (Alvarado et al., 2014), suggesting the buoyancy forces slightly under-estimate the horizontal force acting through the foreland lithosphere in this region. In central Peru, southern Peru, Bolivia, the Puna and high mountains of northern Argentina, where the Andes are 3.8–4.5 km high, the calculated buoyancy forces are 5–6.5 × 10¹² N/m (Figure 4a). In these areas where the buoyancy forces are largest, the high Andes are either undeforming or extending (Mercier et al., 1992; Cladouhos et al., 1994; Lamb, 2000), implying that the buoyancy forces slightly over-estimate the horizontal force acting through the foreland lithosphere. The forces estimated in this study are consistent with previous results for central Peru (2.5–5.0 × 10¹² N/m; see Dalmayrac and Molnar (1981) and Richardson and Coblentz (1994)) and for the Bolivian Altiplano (3.0–6.0 × 10¹² N/m; see Lamb (2000) and Oncken et al. (2012)).

Faults in the forelands will only break in earthquakes if their static frictional resistance to slip is overcome. Therefore, a bound on μ' on faults along the margins of the northern and south-central Andes can be estimated from the condition that the horizontal force supported by the foreland seismogenic layer F_{sl} must be less than F_f in these regions (Copley et al., 2011). The value of μ' represents the effective coefficient of friction averaged over the fault plane and will be an upper bound, as shear zones beneath the brittle faults will also support some of the force acting through the lithosphere.

The horizontal force that can be transmitted through the seismogenic layer of thickness T_s that contains faults that dip at an angle θ relative to the vertical is given by (Turcotte & Schubert, 2002):

$$F_{sl} = \frac{\mu' \rho g T_s^2}{\sin 2\theta - \mu'(1 + \cos 2\theta)}, \tag{1}$$

where g is the acceleration due to gravity and ρ is the average density of the layer. Figure 4b shows the predictions of Equation 1 plotted against estimates of F_f and T_s for the eight different regions of the Andes. In the regions where the foreland seismogenic layer is breaking up in compressional earthquakes on inherited normal faults (Colombia, Ecuador, northern Peru, central Peru and the Puna/Sierra Pampeanas of Argentina), Figure 4b demonstrates that the effective coefficient of friction on these inherited faults is consistently $\mu' < 0.2$, and may well be ≲0.1. This is equivalent to the faults supporting average shear stresses $\bar{\tau} < 150$ MPa in regions with a 45 km thick seismogenic layer and <100 MPa in regions with a 30 km thick seismogenic layer. If the faults were any stronger, the forces acting through the foreland would not be large enough to overcome the frictional resistance to slip and break the seismogenic layer in compressional earthquakes. Notably, where the foreland deformation consists of compressional earthquakes throughout the seismogenic layer, areas with a thicker foreland seismogenic layer support the higher mountain ranges (Maggi, Jackson, McKenzie, & Priestley, 2000).

Around the margins of central Andean plateau in south Peru and Bolivia, where there are no pre-existing normal faults and the foreland is being thrust beneath the mountain range, the relationship between F_f and T_s is less clear (Figure 4b). It is possible that in these regions either: (a) the seismogenic layer is thicker than estimated by the deepest earthquakes, (b) that μ' on any faults is larger than ~0.1–0.2, or (c) that any faults present may be severely mis-oriented relative to the range front strike for re-activation (Figure 4b) (Sibson, 1995). All of
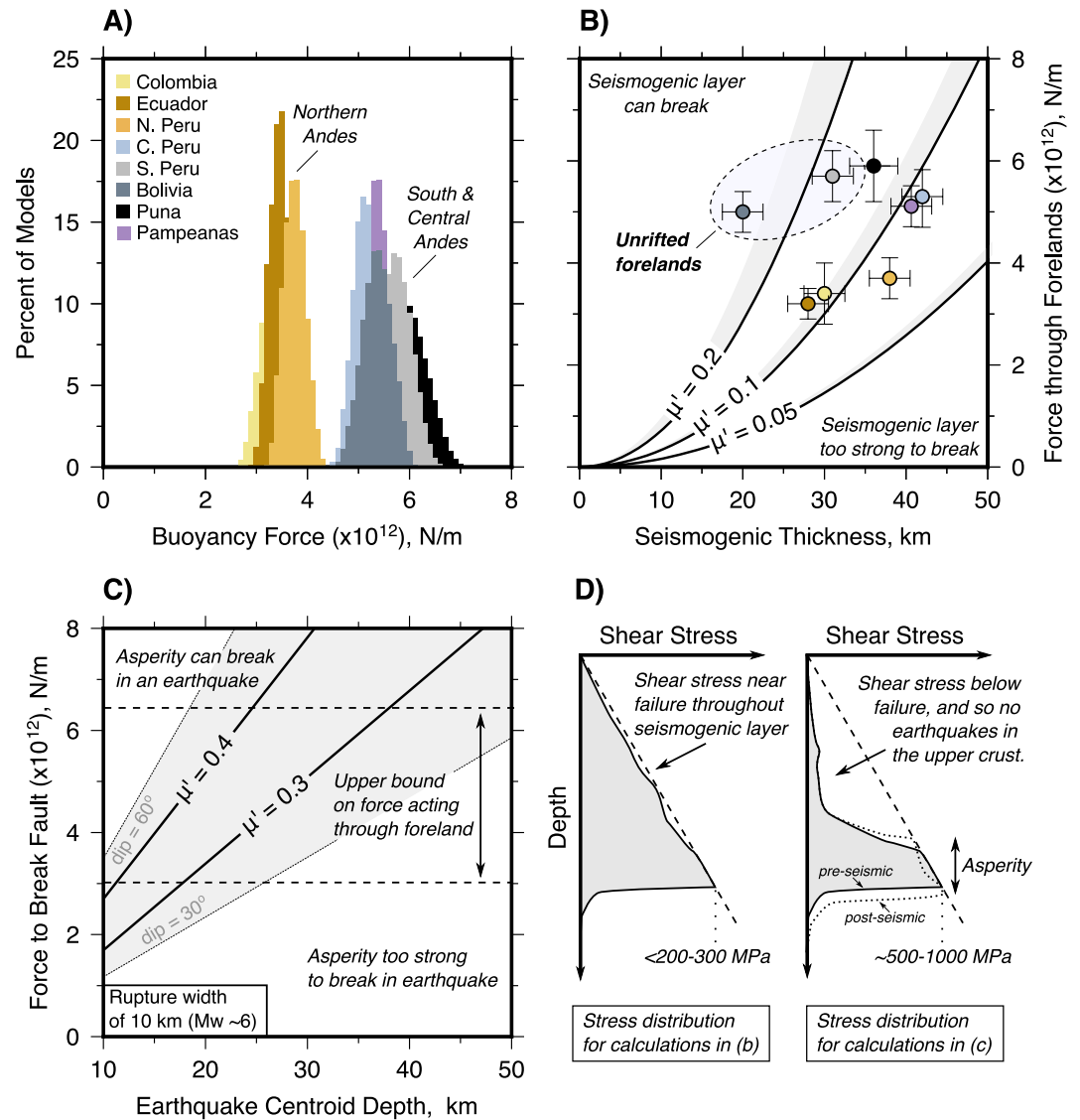
Figure 4. Calculations of the forces acting through the foreland lithosphere and the frictional properties of the foreland faults. (a) Histogram of the buoyancy force F_b acting between the mountains and forelands in seven different regions of the Andes (parameters in Table 2). (b) Seismogenic thickness T_s against the estimate of the force acting through the foreland lithosphere F_f. The uncertainty bars are ± 3 km in T_s and the 95-th percentile of the models in F_f. The thick black lines show the force required to break the seismogenic layer F_{sl} for a given T_s along reverse faults with a $45°$ dip. Gray-shaded regions show the range of F_{sl} for fault dips between $30°$ and $60°$. (c) Calculation for the force required to break fault asperities in the forelands of the Andes in a $M_w \sim 6$ earthquake at a given centroid depth, assuming a dip of $45°$ (thick black lines) or $30–60°$ (gray-shaded region). Horizontal-dashed lines show the force available to break the asperity from (a). (d) Schematic diagram showing the stress distribution with depth along an active fault assumed in the calculations shown in (b) and (c).

these mechanisms would lead to a seismogenic layer that is stronger than the forces acting through the foreland, meaning that the layer is thrust coherently beneath the plateau, as opposed to breaking up through slip on faults. With this configuration of deformation the force transmitted into the mountain range is no longer limited by faults within the foreland lithosphere, but by the strength of faults along the top of the underthrusting foreland and the viscosity of the plateau interior (Babeyko & Sobolev, 2005; Sobolev & Babeyko, 2005).

Many of the earthquakes in the forelands of the northern and south-central Andes are M_w 5–6 and do not necessarily break the full seismogenic layer at any one time. In the locations of these smaller-magnitude earthquakes, the forces acting through the lithosphere may get focused onto strong asperities, whilst the remainder of the fault zone supports shear stresses well below the frictional resistance to slip. The force required to break an asperity

with down-dip width W and centroid depth z_c can be calculated from Equation 1 by replacing the T_s^2 term with $2z_c W \cos\theta$. Even in the extreme case where all of the force acting through the foreland F_f is focused onto the rupture area of a foreland earthquake, the constraints on the size of this force require that $\mu' \lesssim 0.3$–0.4 in order to generate the $M_w \sim 6$ earthquakes near the base of the 30–45 km thick seismogenic layer (Figure 4c). However, the extreme differences in the stress state in the seismogenic layer assumed by this model are unlikely given that strain must accumulate relatively evenly throughout the layer to load and break the faults, and to account for the frequent earthquakes over the seismogenic layer's entire thickness (Figure 4d).

A key result from this analysis is that the size of F_f does not necessarily dictate the style of deformation within the foreland. The foreland seismogenic layer is breaking up in compressional earthquakes both where F_f is its highest (Sierra Pampeanas, central Peru) and its lowest (Ecuador, Colombia). The lack of correlation between F_f and the deformation style implies that enhanced mechanical coupling between the subducting Nazca Plate and overriding South American lithosphere, which is included implicitly in the force-balance analysis (for example, Husson & Ricard, 2004), does not appear to influence the depth extent or pattern of seismicity in the forelands of the Andes.

5. A Dry, Metastable Lower Crust Beneath the Andean Forelands

The frictionally weak faults within the forelands of the northern and south-central Andes remain seismogenic throughout the crust. In this section, I discuss how the depth extent of the seismicity, and the geological history of the inverted rift basins in the forelands, can be used to place constraints on the properties of the lower crust through which these weak faults cut.

A re-assessment of the depth distribution of earthquakes within the continents revealed a bi-modal pattern that depends on the geological history of the region (Maggi, Jackson, Priestley, & Baker, 2000; Jackson, 2002b). Within the young mobile belts (e.g., Tibet, the Aegean, the Basin and Range) faults only remain seismogenic to depths of 10–20 km (Maggi, Jackson, Priestley, & Baker, 2000). The depth extent of seismicity in these settings is thought to be limited by the onset of thermally activated creep in hydrated, quartz-dominated rocks at temperatures of 300–400°C (Sibson, 1982). However, within the Precambrian shield systems that have resisted significant deformation through most of the Phanerozoic (e.g., India, Eurasia, South America), seismicity occurs to depths of 40–60 km, extending through the lower crust and, occasionally, into the upper mantle (Maggi, Jackson, Priestley, & Baker, 2000; Craig et al., 2011; Sloan et al., 2011). Temperatures within the seismogenic lower crust of the Precambrian shields are 400–600°C (McKenzie et al., 2005). Therefore, rocks in the lower crust beneath the Precambrian shields remain seismogenic and mechanically strong, in as much as they resist penetrative deformation and can accumulate and release elastic strain over hundreds of years, to far higher temperatures than beneath the young mobile belts, suggesting that there is some compositional difference between these regions that accounts for their contrasting mechanical properties.

Jackson et al. (2004) argued that the lower crust beneath and along the margins of the Precambrian shields can remain seismogenic at such high temperature because of its anhydrous ("dry") mineralogy. Where sections of the Precambrian lower crust outcrop at the surface, they are typically formed of dry, granulite-facies rocks (Fountain & Salisbury, 1981). These ancient granulites formed as a result of high-temperature (>800–900°C) metamorphism, possibly during mountain building (McKenzie & Priestley, 2016), that stripped the rocks of hydrous minerals through melting (Burton & O'Nions, 1990), leaving behind an anhydrous, load-bearing mineral assemblage of mainly feldspars and pyroxenes. Psuedotachylytes provide evidence that dry granulite can be seismogenic at lower-crustal conditions (Lund et al., 2004; Hawemann et al., 2018), but even trace amounts of water ingress into these rocks leads to viscous creep and mylonite formation that overprints the ancient granulitic fabrics (Austrheim & Boundy, 1994; Menegon et al., 2017). These field observations are consistent with laboratory experiments that show the creep strength of feldspars and pyroxenes is drastically reduced by a few hundredths of a weight percent of structurally bound water at lower-crustal temperatures (Mackwell et al., 1998; Rybacki & Dresen, 2004). Therefore, a seismogenic lower crust, like that beneath the Andean forelands, is often considered to be a proxy for a dry, granulitic lower crust (Sloan et al., 2011; Craig & Jackson, 2021).

The geological history of the crust beneath the Andean forelands can be inferred from inliers and basement-cored reverse faults. Much of this exposed basement is Mesoproterozoic in age (Ramos, 2010a) and has experienced multiple episodes of penetrative deformation and regional metamorphism associated with mountain building and rifting along the western margin of South America (for example, Rapela et al., 1998). The best-exposed

foreland basement can be found in the Sierra Pampeanas, where the most recent high-grade metamorphism and granitic magmatism is dated to two major mountain building episodes in the Cambrian (the Pampean orogeny) and Ordovician-Silurian (the Famatinian orogeny) (Rapela et al., 2010). These orogenies led to granulite-facies metamorphism and melting in the rocks now exposed at the surface, and therefore it is likely the same regional metamorphism will have led to the conditions necessary to form dry, granulitic rocks in the underlying lower crust, which is currently breaking in earthquakes.

Xenoliths provide the most direct evidence for the composition of the lower crust where it is currently seismogenic. The only xenoliths with a clear eruptive origin from the foreland lower crust are found within late Cretaceous basalts that are inter-bedded with the syn-rift sediments of the Metán-Alemania Basin — a sub-basin of the western branch of the Salta Rift (Lucassen et al., 1999) (see Figure 3a for location). The xenolith suite consists of pristine felsic and mafic granulites that equilibrated at temperatures of 800–900°C and pressures of 0.95–1.05 GPa (equivalent to a depth of ∼34–38 km). Peridotite xenoliths in the same suite also record temperatures of 1000–1200°C at pressures of 1.2–1.6 GPa in the shallow lithospheric mantle (Lucassen et al., 2005). Whole-rock Sm-Nd ages of the crustal xenoliths are 80–90 Ma, which are thought to date the timing of their exhumation during syn-rift volcanism (Lucassen et al., 1999). These observations suggest that, in the same depth range there is present-day seismicity beneath the Salta Rift, the lower crust was at granulite-facies conditions in the late Cretaceous (see Figure 2 for depth-range comparison).

Present-day conditions within the lower crust beneath the Salta Rift will be lower in pressure and temperature than those during rifting, as a result of the thinning of the radiogenic crust and conductive cooling of the lithosphere (Sandiford & Powell, 1986). To estimate the evolution of the P–T conditions beneath the Salta Rift, I ran a series of numerical calculations that simulate the late Cretaceous rifting and subsequent post-rift cooling based on the 1-D thermo-kinematic numerical model of Bown and White (1995) (see Text S2 in Supporting Information S1 for details of the model set-up). I used a grid-search approach to find models that matched the P–T–t constraints from xenolith thermobarometry, the history of syn- and post-rift sedimentation within the Metán-Alemania basin (Salfity & Marquillas, 1994; Starck, 2010), and the present-day crust and lithospheric mantle thickness. I then used the models that fit these varied data to explore the possible P–T–t evolution of the seismogenic lower crust (Figure 5).

During rifting, the geotherm was perturbed away from a steady state and rocks were advected toward the surface causing a pressure decrease (ΔP). The amplitude of ΔP is controlled primarily by the amount of crustal stretching. At this time the lower crust was hot enough to undergo the dehydration-melting reactions necessary to form granulite-facies rocks at depths of ∼35 km (Figure 5a). The high lower-crustal temperatures could be achieved in the modeling by significant syn-rift thinning of the lithospheric mantle (for example, Hopper et al., 2020), or an initially hot geotherm due to a thick radiogenic crust or thin lithospheric mantle. However, the limited amount of felsic magmatism recorded within the syn-rift sediments (Salfity & Marquillas, 1994) implies that the lower crust was already mostly dry by the Cretaceous in order to avoid widespread melting. Subsequent post-rift cooling over ∼80–90 Myrs led to a decrease in temperature (ΔT) throughout the lower crust. For rocks exhumed to a depth of 35 km, the models estimate that ΔT = 75–250°C and ΔP = 0.15–0.25 GPa (Figures 5b and 5c). Estimates of the present-day temperatures at 35 km depth beneath the Salta Rift are 600–700°C (Figure 5a), with the lower crust still cooling toward steady state.

The xenolith data and rift models suggest that, if the lower crust beneath the western branch of the Salta Rift was not already formed of dry granulite, then the P-T conditions in the late Cretaceous will have led to widespread granulite-facies metamorphism. A modern analogue of the Cretaceous Salta Rift may be the Rio Grande Rift, where young crustal xenoliths also record granulite-facies conditions at the base of the lower crust (Cipar et al., 2020). The lower crust has subsequently cooled to amphibolite-facies conditions. Despite the significant changes in P and T, the dry granulites within the lower crust are likely to have remained metastable, as the possible retrograde reactions have sluggish kinetics in the absence of the volatiles that were driven off by melting and melt segregation along their prograde path (Brown, 2002). The geological evolution of the Salta Rift is therefore consistent with the view that, where the lower crust is seismogenic along the margins of the Andes, it is formed of dry, granulitic rocks that preserve a metastable mineral assemblage (Jackson et al., 2021). Nonetheless, more xenolith data that sample sections of the foreland lower crust along the remainder of the Andean range front are needed to rigorously test this hypothesis.
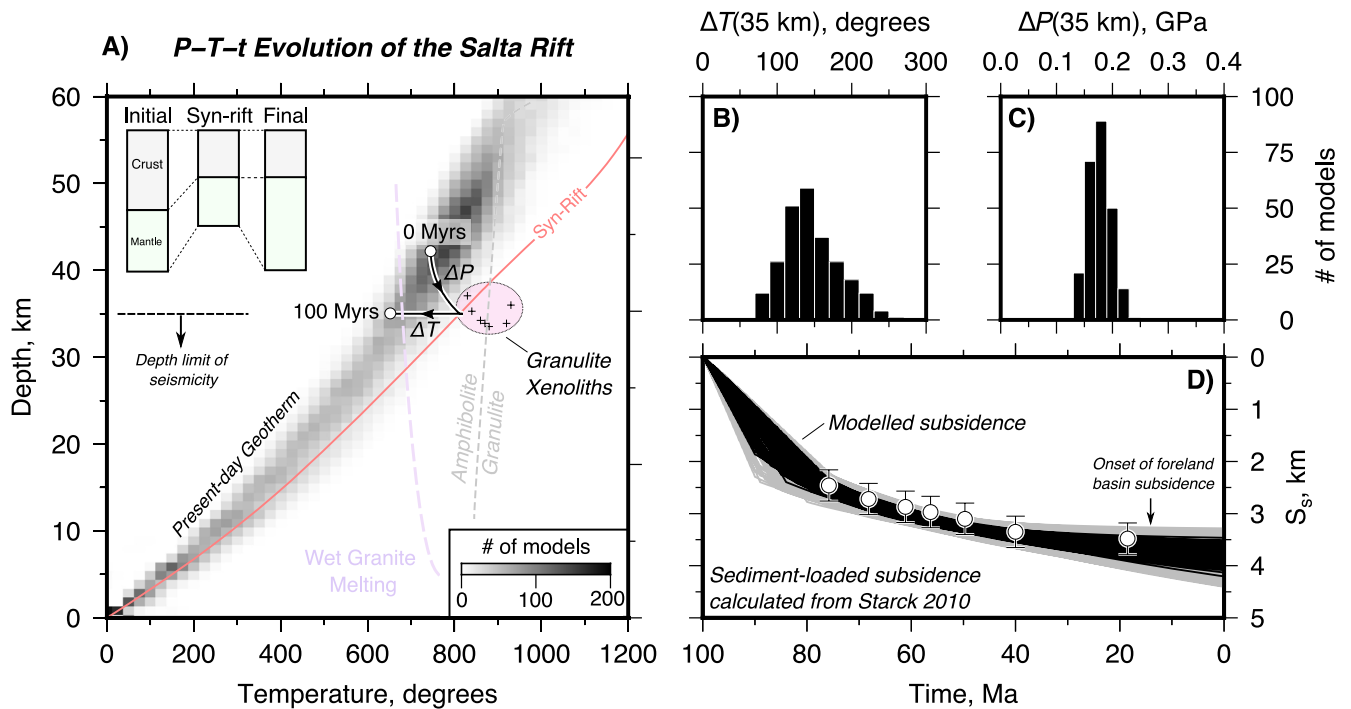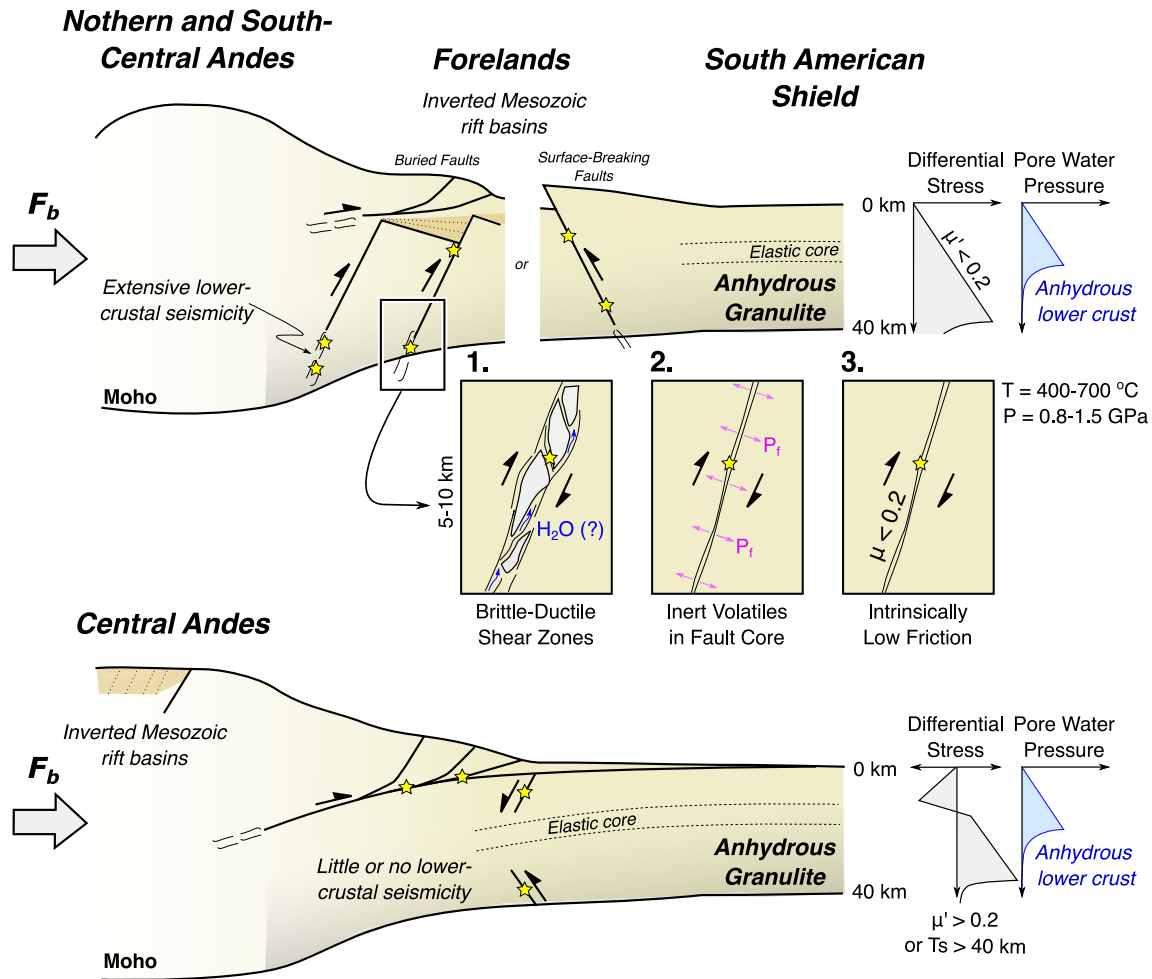
Figure 5. Theoretical estimates of the pressure-temperature-time (*P-T-t*) evolution for rocks in the lower crust beneath the Salta Rift calculated using thermo-kinematic models that fit the sediment-loaded subsidence history within the Metán-Alemania Basin and the temperature constraints from xenolith thermobarometry. (a) Example *P-T-t* history for rocks exhumed to 35 km depth (black line) and the associated syn-rift geotherm (light red line) from one particular model. The range of possible present-day geotherms is shown by the density plot in the background, which is calculated from all of the models that match the geological constraints and the observed subsidence history (S_s) to within $\chi^2 < 3$ (see Text S2 in Supporting Information S1). (b) Distribution of the temperature decrease ΔT for a rock volume exhumed to 35 km depth, and (c) distribution of the equivalent pressure decrease ΔP assuming a crustal density of 2,800 kg/m^3. (d) Decompacted sediment-loaded subsidence history (S_s) in the Metán-Alemania Basin from Starck (2010) (white dots) and the model predictions (S_m). Black lines = models that fit to within $\chi^2 < 1$, gray lines = models that fit to within $\chi^2 < 3$.

6. Discussion

6.1. Structural Inheritance and Mountain Building in the Andes

Watts et al. (1995) first recognised that there is a link between the pattern of active deformation along the margins of the Andes, the mechanical properties of the foreland lithosphere and the first-order shape of the high mountains. They demonstrated that foreland lithosphere surrounding the wide and curved central Andean plateau has a high effective elastic thickness and is overlain by a thin-skinned fold-thrust belt that has accommodated extensive (60–120 km) Late Miocene-Recent shortening. In contrast, the narrow and linear ranges of the northern and south-central Andes have a foreland lithosphere with a lower effective elastic thickness that is breaking up along steeply dipping faults that have accommodated less Late Miocene-Recent shortening (see also Kley & Monaldi, 1998; Oncken et al., 2006). These observations led Watts et al. (1995) to suggest that along-strike differences in the mechanical properties of the foreland lithosphere control the style of deformation in the forelands, and that these variations in deformation style may, in turn, have influenced the Late Miocene-Recent growth of the Andes.

This study provides new insight into how the mechanical properties of the foreland lithosphere and the style of active deformation are linked. I have shown that, where Mesozoic rifts lie along the range front in the northern and south-central Andes, the foreland crust is highly seismogenic and is deforming entirely in compressional earthquakes (Figure 6, top). Frictionally weak faults inherited from the rifts cut through the crust and are accommodating a significant component of the shortening, though these faults can be obscured at the surface by aseismic fold-thrust belts formed in the sedimentary cover (e.g., Marañon basin of central Peru). In contrast, where the Mesozoic rifts are absent from beneath the range front around the central Andean plateau, the foreland crust has experienced far fewer earthquakes, which mainly have shallow thrust-faulting mechanisms beneath the range front and normal-faulting mechanisms further into the foreland. The seismicity around the plateau is consistent

Figure 6. Sketches of the two contrasting styles of shortening in the forelands of the northern and south-central Andes (top) and the central Andes (bottom), adapted from Figure 7 in Watts et al. (1995). In the northern and south-central Andes, frictionally weak faults inherited from Mesozoic rift systems that cut through the lower crust are breaking in earthquakes down to ~40–45 km depth. Three different mechanical explanations for how these deep faults may be both seismogenic and frictionally weak are shown, with each of these mechanisms being consistent with a dry lower crust beneath the Andean forelands. Along the margins of the central Andean plateau, there has been little or no recent seismicity in the lower crust, and the foreland is thought to underthrusting the high plateau. In this area the Mesozoic rift basins can be identified within the interior of the mountain range. The top of the foreland crust is in extension and its base is in compression, suggesting the seismogenic layer is bending beneath the mountains.

with the view that the foreland seismogenic layer is too strong to break up in compression, so is bending and underthrusting the mountain range coherently beneath a low-angle décollement (Allmendinger & Gubbels, 1996) (Figure 6, bottom). Whether the forelands of the Andes can break up, or whether they underthrust the mountains, is therefore controlled by the effects of Mesozoic rifting on the mechanical properties of the foreland seismogenic layer.

Notably, the thickness of the seismogenic layer in the forelands does not correlate with the deformation style (see Section 4). Therefore, the thermal effects of Mesozoic rifting (for example, Stewart & Watts, 1997) or Miocene-Pliocene volcanism (for example, Ramos et al., 2002) do not appear to have created a thinner seismogenic layer in the northern and south-central Andes that is easier to break. Similarly, along-strike changes in the thickness of the foreland lithosphere determined from surface-wave tomography (for example, Priestley & McKenzie, 2013; Celli et al., 2020) do not appear to correlate with the deformation style (Figure 3 in Supporting Information S1). Although, the horizontal resolution of the tomography (~100–300 km), and the possibility of horizontal smearing of velocity anomalies associated with the subducting Nazca Plate, precludes any confident comparison of lithospheric thickness and deformation style. The explanation that is most consistent with the observations available is that Mesozoic rifting formed or reactivated frictionally weak, range-parallel

faults along the western margin of the Precambrian shields and accreted terranes of South America. As these regions are shortened, the presence or absence of weak faults that are well-oriented relative to the range front for failure control the strength of the seismogenic layer and therefore the style of foreland deformation. The presence of mechanically weak sediments on top of the foreland basement (Allmendinger & Gubbels, 1996) and viscous resistance to underthrusting beneath the Andes (Babeyko & Sobolev, 2005) may play a secondary role in controlling the style of foreland deformation.

6.2. Weak, Seismogenic Faults in a Dry Lower Crust

The force-balance calculations presented in Section 4 demonstrated that faults within the forelands of the northern and south-central Andes are frictionally weak compared to laboratory experiments of static friction, and yet remain able to generate earthquakes at unusually high temperatures of $\sim$400–700°C in the lower crust. The lower crust is thought to be extremely dry in order to remain seismogenic at such high temperatures (Jackson et al., 2004). Two mechanisms have been invoked to account for frictionally weak faults in the upper crust: (a) highly pressurized water within the fault core, and (b) intrinsically weak phyllosilicate minerals within faults that are produced through water-mediated alteration of the fault rock. In this section, I critically assess whether the same, water-mediated mechanisms weakening faults in the upper crust could control the frictional properties of seismogenic faults in the lower crust.

First, the dry and granulitic wall rocks inferred to surround faults in the forelands of the Andes will be metastable at lower-crustal conditions, and will readily react with free water to form new, stable mineral assemblages. The composition of the lower crust should therefore act as a sink of water and buffer the water pressure to far below lithostatic over time, except in regions of pervasive water influx and retrogression (Yardley & Valley, 1997). The rates of hydration reactions from natural analogs suggest water can be consumed by dry granulitic rocks at mid-crustal temperature conditions at $\sim$10^{-8} g/cm^2/s (Whyte et al., 2021). Without some mechanism that can isolate free water within the fault core from the reactive wall rocks, it is therefore unlikely that a pervasive water phase within the fault zone at 60%–80% of lithostatic pressure is the cause of the frictionally weak faults in the lower crust.

If water influx does occur into a fault zone formed of dry granulite at amphibolite-facies conditions, it will lead to water-consuming reactions that form hydrous minerals, particularly amphiboles and phyllosilicates (for example, Beach, 1976; Andersen et al., 1991). A common feature of exhumed granulite terrains are shear zones that contain aligned hydrous minerals surrounded by anhydrous wall rocks that preserve ancient fabrics (for example, Sørensen, 1983; Newton, 1990; Austrheim & Boundy, 1994; Getsinger et al., 2013; Menegon et al., 2017). This widespread observation implies that water ingress into fault zones during deformation leads to localized reaction softening along the fault and the onset of viscous creep at lower-crustal conditions, precluding the accumulation of elastic strain and frictional slip. The seismogenic fault zones in the Andean forelands are interpreted to have been re-activated following Mesozoic rifting, and presumably have a protracted history of deformation over millions of years that would have caused localized water ingress and reaction softening if there was water available in the lower crust. Therefore an alternative, water-absent mechanism may be necessary to account for the frictional properties of faults within the lower crust of the Andean forelands. Below I discuss some possible alternatives.

Shear zones within lower-crustal terrains often form networks of fine-grained or hydrated rocks in outcrop that wrap around rigid, undeformed blocks (for example, Sørensen, 1983). It is possible that earthquakes nucleate at stress concentrations in these mechanically heterogeneous fault zones by rupturing the rigid blocks (Figure 6, box 1). Although this mechanism can certainly account for small earthquakes (Campbell et al., 2020), for moderate-magnitude earthquakes with kilometer-sized rupture areas like those in the Andean forelands, even if all of the force acting through the lithosphere were focused onto the rupture area, the faults must still have an effective coefficient of friction less than half that predicted by Byerlee's Law (see the calculations presented in Section 4). Otherwise, the faults within the rigid blocks would be too strong to break, given the constraints on the size of the force acting through the foreland lithosphere.

Alternatively, fluids rich in non-hydrous volatile phases (e.g., N_2, CO_2) may be present as inter-granular films and in pores in lower-crustal fault zones (Andersen et al., 1990). Non-hydrous volatiles can reduce the activity of water in any fluid that may exist, which helps stabilize the anhydrous mineral assemblage of granulites that is

needed for elastic strain to accumulate at high temperatures. The volatiles may also become highly pressurized through deformation compaction and reduce the effective stresses within the fault zone without lowering the creep strength of the rock (Figure 6, box 2). Few experimental constraints exist on the influence of non-hydrous volatiles on creep in silicate minerals, which limits any quantitative test of this mechanism. Nonetheless, evidence from exhumed psuedotachylytes suggest that CO_2-rich fluids are associated with frictional slip in mafic granulites at lower-crustal conditions (Sørensen et al., 2019).

It is also possible that the conditions under which friction is measured in the laboratory are just too far removed from those experienced by lower-crustal fault zones, and that dry fault rocks are intrinsically frictionally weak at high confining pressures and temperatures (Figure 6, box 3). For example, if frictional resistance is governed by microscopic surface roughness, then the high temperatures and long inter-event times in the lower crust may allow asperities on fault surfaces to relax through localized creep, producing smooth and frictionally weak faults. This explanation circumvents the need for a free fluid phase all together, and would account for the observation that psuedotachylytes can occur in completely dry lower-crustal rocks (Hawemann et al., 2019; Dunkel et al., 2021). However, the same asperity relaxation effects have been shown to cause a transition from velocity-weakening (i.e., seismogenic) to velocity-strengthening (i.e., aseismic) slip behavior in olivine aggregates deformed at high temperatures (Boettcher et al., 2007), which may in fact preclude lower-crustal seismicity.

It therefore remains unclear which, if any, of these mechanisms may account for the frictional properties of faults in the Andean forelands. Testing the different hypotheses shown in Figure 6 using geological observations is difficult, as the various mechanisms are highly dependent on the mineralogy, fluid availability and fluid composition, which will all vary along the fault. In contrast, the geophysical constraints developed in this study reflect fault-averaged frictional properties over length-scales of kilometres, which undoubtedly smooth out complex, outcrop-scale structure and processes. Further measurements of the frictional strength of faults in various geological settings, with different deformation rates and over different length-scale, are needed to understand what controls their effective strength. Nonetheless, a few simple conclusions regarding the mechanics of lower-crustal fault zones can be drawn from this discussion: (a) frictionally weak faults may remain seismogenic in the continental lower crust after multiple episodes of reactivation separated by millions of years, and (b) water-assisted weakening mechanisms like those inferred to be active in the upper crust are unlikely to operate on seismogenic, lower-crustal faults if they are surrounded by dry and metastable rocks.

7. Conclusions

I have shown that the distribution of seismicity along the margin of the Andes is correlated with the locus of Mesozoic rift systems that stretched the foreland lithosphere prior to the Andean orogeny. Where the rift systems lie along the margins of the mountain belt, the whole 30–45 km-thick seismogenic layer is shortening by slip on inherited normal faults. Where these inherited faults are absent, or mis-oriented relative to the shortening direction, the foreland is bending and being underthrust beneath the Andes. I have estimated the forces acting on the inherited faults, and demonstrated that they have an effective coefficient of static friction $\mu' < 0.2$, which is significantly lower than predicted by laboratory experiments. The mechanisms that have been proposed to generate weak, seismogenic faults in the upper crust are typically related to a free water-phase. I argue that these water-assisted mechanisms alone are unlikely to weaken faults in the seismogenic lower crust due to its dry, granulitic composition and the effect of water on viscous creep mechanisms at high temperatures. Therefore, although the frictional properties of faults within the Andean forelands appear to be important in controlling the style of mountain building, the geological controls on their mechanical properties remain enigmatic.

Data Availability Statement

Waveform data used in this study was is freely available from the Incorporated Research Institute for Seismology (IRIS) data management centre. The computer codes used to perform the force-balance calculations and the 1-D thermo-kinematic modelling are available from: https://doi.org/10.5281/zenodo.6112269. All earthquake focal mechanism data will be uploaded to the gWFM catalogue available at: https://comet.nerc.ac.uk/gwfm_catalogue/gWFM_catalogue.html.

References

Allmendinger, R., & Gubbels, T. (1996). Pure and simple shear plateau uplift, Altiplano-Puna, Argentina and Bolivia. *Tectonophysics*, *259*(1–3), 1–13. https://doi.org/10.1016/0040-1951(96)00024-8

Alvarado, A., Audin, L., Nocquet, J. M., Lagreulet, S., Segovia, M., Font, Y., et al. (2014). Active tectonics in Quito, Ecuador, assessed by geomorphological studies, GPS data, and crustal seismicity. *Tectonics*, *33*(2), 67–83. https://doi.org/10.1002/2012tc003224

Alvarado, P., & Beck, S. (2006). Source characterization of the San Juan (Argentina) crustal earthquakes of 15 january 1944 (Mw 7.0) and 11 june 1952 (Mw 6.8). *Earth and Planetary Science Letters*, *243*(3–4), 615–632. https://doi.org/10.1016/j.epsl.2006.01.015

Alvarado, P., Beck, S., Zandt, G., Araujo, M., Triep, E., Isacks, B. L., et al. (2005). Crustal deformation in the south-central Andes backarc terranes as viewed from regional broad-band seismic waveform modelling. *Geophysical Journal International*, *163*(2), 580–598. https://doi.org/10.1111/j.1365-246x.2005.02759.x

Andersen, T., Austrheim, H., & Burke, E. A. (1991). Fluid-induced retrogression of granulites in the Bergen Arcs, Caledonides of W. Norway: Fluid inclusion evidence from amphibolite-facies shear zones. *Lithos*, *27*(1), 29–42. https://doi.org/10.1016/0024-4937(91)90018-g

Andersen, T., Austrheim, H., & Burke, E. A. J. (1990). Fluid inclusions in granulites and eclogites from the bergen arcs, caledonides of W. Norway. *Mineralogical Magazine*, *54*(375), 145–158. https://doi.org/10.1180/minmag.1990.054.375.02

Assumpção, M., & Araujo, M. (1993). Effect of the Altiplano-Puna plateau, South America, on the regional intraplate stresses. *Tectonophysics*, *221*(3–4), 475–496. https://doi.org/10.1016/0040-1951(93)90174-i

Assumpção, M., Feng, M., Tassara, A., & Julià, J. (2013). Models of crustal thickness for South America from seismic refraction, receiver functions and surface wave tomography. *Tectonophysics*, *609*, 82–96. https://doi.org/10.1016/j.tecto.2012.11.014

Assumpção, M., & Suarez, G. (1988). Source mechanisms of moderate-size earthquakes and stress orientation in mid-plate South America. *Geophysical Journal International*, *92*(2), 253–267. https://doi.org/10.1111/j.1365-246x.1988.tb01138.x

Austrheim, H., & Boundy, T. M. (1994). Pseudotachylytes generated during seismic faulting and eclogitization of the deep crust. *Science*, *265*(5168), 82–83. https://doi.org/10.1126/science.265.5168.82

Babeyko, A. Y., & Sobolev, S. V. (2005). Quantifying different modes of the late Cenozoic shortening in the central Andes. *Geology*, *33*(8), 621–624. https://doi.org/10.1130/g21126ar.1

Barke, R., Lamb, S., & MacNiocaill, C. (2007). Late Cenozoic bending of the Bolivian Andes: New paleomagnetic and kinematic constraints. *Journal of Geophysical Research: Solid Earth*, *112*(1), 1–22. https://doi.org/10.1029/2006jb004372

Beach, A. (1976). The interrelations of fluid transport, deformation, geochemistry and heat flow in early proterozoic shear zones in the lewisian complex author (s): A Beach source: philosophical transactions of the royal society of London. Series A, *Mathematical Philosophical Transactions of the Royal Society A.* (Vol. *280*(1298), pp. 569–604).

Boettcher, M. S., Hirth, G., & Evans, B. (2007). Olivine friction at the base of oceanic seismogenic zones. *Journal of Geophysical Research: Solid Earth*, *112*(1), 1–13. https://doi.org/10.1029/2006jb004301

Bown, J. W., & White, R. S. (1995). Effect of finite extension rate on melt generation at rifted continental margins. *Journal of Geophysical Research*, *100*(B9), 18011–18029. https://doi.org/10.1029/94jb01478

Brooks, B. a., Bevis, M., Whipple, K., Ramon Arrowsmith, J., Foster, J., Zapata, T., et al. (2011). Orogenic-wedge deformation and potential for great earthquakes in the central Andean backarc. *Nature Geoscience*, *4*(6), 380–383. https://doi.org/10.1038/ngeo1143

Brown, M. (2002). Retrograde processes in migmatites and granulites revisited. *Journal of Metamorphic Geology*, *20*(1), 25–40. https://doi.org/10.1046/j.0263-4929.2001.00362.x

Burton, K. W., & O'Nions, R. K. (1990). The timescale and mechanism of granulite formation at Kurunegala, Sri Lanka. *Contributions to Mineralogy and Petrology*, *106*(1), 66–89. https://doi.org/10.1007/bf00306409

Butler, R. W., Tavarnelli, E., & Grasso, M. (2006). Structural inheritance in mountain belts: An Alpine-Apennine perspective. *Journal of Structural Geology*, *28*(11), 1893–1908. https://doi.org/10.1016/j.jsg.2006.09.006

Byerlee, J. (1978). Friction of rocks. *Pure and Applied Geophysics*, *116*(4–5), 615–626. https://doi.org/10.1007/978-3-0348-7182-2_4

Cahill, T., Isacks, B. L., Whitman, D., Chatelain, J. L., Perez, A., & Chiu, J. M. (1992). Seismicity and tectonics in jujuy province, northwestern Argentina. *Tectonics*, *11*(5), 944–959. https://doi.org/10.1029/92tc00215

Campbell, L. R., Menegon, L., Fagereng, Å., & Pennacchioni, G. (2020). Earthquake nucleation in the lower crust by local stress amplification. *Nature Communications*, *11*(1), 1–9. https://doi.org/10.1038/s41467-020-15150-x

Celli, N. L., Lebedev, S., Schaeffer, A. J., Ravenna, M., & Gaina, C. (2020). The upper mantle beneath the South Atlantic Ocean, South America and Africa from waveform tomography with massive data sets. *Geophysical Journal International*, *221*(1), 178–204. https://doi.org/10.1093/gji/ggz574

Charrier, R., Ramos, V. A., Tapia, F., & Sagripanti, L. (2015). *Tectono-stratigraphic Evolution of the Andean Orogen between 31 and 37S (Chile and Western Argentina)* (Vol. 399, pp. 13–61). Geological Society Special Publication.

Chinn, D. S., & Isacks, B. L. (1983). Accurate source depths and focal mechanisms of shallow earthquakes in Western South America and in the New Hebrides Island Arc. *Tectonics*, *2*(6), 529–563. https://doi.org/10.1029/tc002i006p00529

Cipar, J. H., Garber, J. M., Kylander-Clark, A. R., & Smye, A. J. (2020). Active crustal differentiation beneath the Rio Grande Rift. *Nature Geoscience*, *13*(11), 758–763. https://doi.org/10.1038/s41561-020-0640-z

Cladouhos, T. T., Allmendinger, R. W., Coira, B., & Farrar, E. (1994). Late cenozoic deformation in the central Andes: Fault kinematics from the northern Puna, northwestern Argentina and southwestern Bolivia. *Journal of South American Earth Sciences*, *7*(2), 209–228. https://doi.org/10.1016/0895-9811(94)90008-6

Coira, B., Davidson, J., Mpodozis, C., & Ramos, V. (1982). Tectonic and magmatic evolution of the Andes of northern Argentina and Chile. *Earth-Science Reviews*, *18*(3–4), 303–332. https://doi.org/10.1016/0012-8252(82)90042-3

Collettini, C., Tesei, T., Scuderi, M. M., Carpenter, B. M., & Viti, C. (2019). Beyond Byerlee friction, weak faults and implications for slip behavior. *Earth and Planetary Science Letters*, *519*, 245–263. https://doi.org/10.1016/j.epsl.2019.05.011

Condori, C., França, G. S., Tavera, H. J., Albuquerque, D. F., Bishop, B. T., & Beck, S. L. (2017). Crustal structure of north Peru from analysis of teleseismic receiver functions. *Journal of South American Earth Sciences*, *76*, 11–24. https://doi.org/10.1016/j.jsames.2017.02.006

Copley, A. (2018). The strength of earthquake-generating faults. *Journal of the Geological Society*, *174*(1)–12. https://doi.org/10.1144/jgs2017-037

Copley, A., Avouac, J.-P., Hollingsworth, J., & Leprince, S. (2011). The 2001 Mw 7.6 Bhuj earthquake, low fault friction, and the crustal support of plate driving forces in India. *Journal of Geophysical Research: Solid Earth*, *116*(B8), B08405. https://doi.org/10.1029/2010jb008137

Copley, A., & Woodcock, N. (2016). Estimates of fault strength from the Variscan foreland of the northern UK. *Earth and Planetary Science Letters*, *451*, 108–113. https://doi.org/10.1016/j.epsl.2016.07.024

Craig, T. J., Copley, A., & Jackson, J. A. (2012). Thermal and tectonic consequences of India underthrusting Tibet. *Earth and Planetary Science Letters*, *353–354*, 231–239. https://doi.org/10.1016/j.epsl.2012.07.010

Craig, T. J., & Jackson, J. A. (2021). Variations in the seismogenic thickness of east Africa. *Journal of Geophysical Research: Solid Earth*, *126*(3), e2020JB020754. https://doi.org/10.1029/2020jb020754

Craig, T. J., Jackson, J. A., Priestley, K., & McKenzie, D. (2011). Earthquake distribution patterns in Africa: Their relationship to variations in lithospheric and geological structure, and their rheological implications. *Geophysical Journal International*, *185*(1), 403–434. https://doi.org/10.1111/j.1365-246x.2011.04950.x

Dalmayrac, B., & Molnar, P. (1981). Parallel thrust and normal faulting in Peru and constraints on the state of stress. *Earth and Planetary Science Letters*, *55*(3), 473–481. https://doi.org/10.1016/0012-821x(81)90174-6

Devlin, S., Isacks, B. L., Pritchard, M. E., Barnhart, W. D., & Lohman, R. B. (2012). Depths and focal mechanisms of crustal earthquakes in the central Andes determined from teleseismic waveform analysis and InSAR. *Tectonics*, *31*(2), 1–33. https://doi.org/10.1029/2011tc002914

Dimate, C., Rivera, L., Taboada, A., Delouis, B., Osorio, A., Jimenez, E., et al. (2003). The 19 January 1995 Tauramena (Colombia) earthquake: Geometry and stress regime. *Tectonophysics*, *363*(3–4), 159–180. https://doi.org/10.1016/s0040-1951(02)00670-4

Dorbath, C., Dorbath, L., Cisternas, A., Deverchere, J., Diament, M., Ocola, L., & Morales, M. (1986). On crustal seismicity of the Amazonian foothill of the central Peruvian Andes. *Geophysical Research Letters*, *13*(10), 1023–1026. https://doi.org/10.1029/gl013i010p01023

Dunkel, K. G., Zhong, X., Arnestad, P. F., Valen, L. V., & Jamtveit, B. (2021). High transient stress in the lower crust: Evidence from dry pseudotachylytes in granulites, lofoten archipelago, northern Norway. *Geology*, *49*(2), 135–139. https://doi.org/10.1130/g48002.1

Fountain, D. M., & Salisbury, M. H. (1981). Exposed cross-sections through the continental crust: Implications for crustal structure, petrology, and evolution. *Earth and Planetary Science Letters*, *56*(C), 263–277. https://doi.org/10.1016/0012-821x(81)90133-3

Getsinger, A. J., Hirth, G., Stünitz, H., & Goergen, E. T. (2013). Influence of water on rheology and strain localization in the lower continental crust. *Geochemistry, Geophysics, Geosystems*, *14*(7), 2247–2264. https://doi.org/10.1002/ggge.20148

Golonka, J., Lawver, L., Coffin, M., Dalziel, I. D., & Gahagan, L. (1995). *Paleogeographic reconstructions with sediment isopachs, PLATES progress report No. 104-0695*. Technical report. University of Texas Institute for Geophysics.

Gubbels, T. L., Isacks, B. L., & Farrar, E. (1993). High-level surfaces, plateau uplift, and foreland development, Bolivian central Andes. *Geology*, *21*(8), 695. https://doi.org/10.1130/0091-7613(1993)021<0695:hlspua>2.3.co;2

Gutscher, M.-A., Spakman, W., Bijwaard, H., & Enghdahl, E. R. (2000). Geodynamics of flat subduction: Seismicity and tomographic constraints from the Andean margin. *Tectonics*, *19*(5), 814–833. https://doi.org/10.1029/1999tc001152

Hawemann, F., Mancktelow, N. S., Pennacchioni, G., Wex, S., & Camacho, A. (2019). Weak and slow, strong and fast: How shear zones evolve in a dry continental crust (musgrave ranges, central Australia). *Journal of Geophysical Research: Solid Earth*, *124*(1), 219–240. https://doi.org/10.1029/2018jb016559

Hawemann, F., Mancktelow, N. S., Wex, S., Camacho, A., & Pennacchioni, G. (2018). Pseudotachylyte as field evidence for lower-crustal earthquakes during the intracontinental petermann orogeny (musgrave block, central Australia). *Solid Earth*, *9*(3), 629–648. https://doi.org/10.5194/se-9-629-2018

Hayes, G. P., Moore, G. L., Portner, D. E., Hearne, M., Flamme, H., Furtney, M., & Smoczyk, G. M. (2018). Slab2, a comprehensive subduction zone geometry model. *Science*, *362*(6410), 58–61. https://doi.org/10.1126/science.aat4723

Hermoza, W., Brusset, S., Baby, P., Gil, W., Roddaz, M., Guerrero, N., & Bolaños, M. (2005). The Huallaga foreland basin evolution: Thrust propagation in a deltaic environment, northern Peruvian Andes. *Journal of South American Earth Sciences*, *19*(1), 21–34. (SPEC. ISS.). https://doi.org/10.1016/j.jsames.2004.06.005

Hopper, E., Gaherty, J. B., Shillington, D. J., Accardo, N. J., Nyblade, A. A., Holtzman, B. K., et al. (2020). Preferential localized thinning of lithospheric mantle in the melt-poor Malawi Rift. *Nature Geoscience*, *13*(8), 584–589. https://doi.org/10.1038/s41561-020-0609-y

Hubbert, M. K., & Rubey, W. W. (1959). Mechanics of fluid-filled porous solids and its application to overthrust faulting. *Bulletin of the Geological Society of America*, *70*(2), 115–166.

Husson, L., & Ricard, Y. (2004). Stress balance above subduction: Application to the Andes. *Earth and Planetary Science Letters*, *222*(3–4), 1037–1050. https://doi.org/10.1016/s0012-821x(04)00235-3

Imber, J., Holdsworth, R. E., Butler, C. A., & Lloyd, G. E. (1997). Fault-zone weakening processes along the reactivated outer hebrides fault zone, scotland. *Journal of the Geological Society*, *154*(1), 105–109. https://doi.org/10.1144/gsjgs.154.1.0105

Jackson, J. (2002). Faulting, flow, and the strength of the continental lithosphere. *International Geology Review*, *44*(1), 39–61. https://doi.org/10.2747/0020-6814.44.1.39

Jackson, J., McKenzie, D., & Priestley, K. (2021). Relations between earthquake distributions, geological history, tectonics and rheology on the continents. *Philosophical Transactions of the Royal Society A: Mathematical, Physical & Engineering Sciences*, *379*(2193). https://doi.org/10.1098/rsta.2019.0412

Jackson, J. A. (2002). Strength of the continental lithosphere: Time to abandon the jelly sandwich? *Geological Society of America Today*, *12*(9), 4. https://doi.org/10.1130/1052-5173(2002)012<0004:sotclt>2.0.co;2

Jackson, J. A., Austrheim, H., McKenzie, D., & Priestley, K. (2004). Metastability, mechanical strength, and the support of mountain belts. *Geology*, *32*(7), 625. https://doi.org/10.1130/g20397.1

Jordan, T. E., Isacks, B. l., Allmendinger, R. E., Brewer, J. A., Ramos, V. A., & Ando, C. J. (1983). Andean tectonics related to geometry of subducted Nazca plate. *The Geological Society of America Bulletin*, *94*(3), 341. https://doi.org/10.1130/0016-7606(1983)94<341:atrtgo>2.0.co;2

Kadinsky-Cade, K., Reilinger, R., & Isacks, B. (1985). Surface deformation associated with the November 23, 1977, Caucete, Argentina, earthquake sequence. *Journal of Geophysical Research: Solid Earth*, *90*(14), 12691–12700. https://doi.org/10.1029/jb090ib14p12691

Kendrick, E., Bevis, M., Smalley, R., & Brooks, B. (2001). An integrated crustal velocity field for the central Andes. *Geochemistry, Geophysics, Geosystems*, *2*(11). https://doi.org/10.1029/2001gc000191

Kendrick, E., Brooks, B. A., Bevis, M. R. S., Jr, Lauria, E., Araujo, M., & Parra, H. (2006). Orogenia activa de los Andes centro-australes estudiada mediante geodesia de GPS. *Revista de la Asociación Geológica Argentina*, *61*(4), 555–566.

Kennan, L., Lamb, S. H., & Hoke, L. (1997). High-altitude palaeosurfaces in the Bolivian Andes: Evidence for late cenozoic surface uplift. *Geological Society, London, Special Publications*, *120*(1), 307–323. https://doi.org/10.1144/gsl.sp.1997.120.01.20

Kley, J., & Monaldi, C. R. (1998). Tectonic shortening and crustal thickness in the Central Andes: How good is the correlation? *Geology*, *26*(8), 723–726. https://doi.org/10.1130/0091-7613(1998)026<0723:tsacti>2.3.co;2

Kley, J., & Monaldi, C. R. (2002). Tectonic inversion in the Santa Barbara System of the central Andean foreland thrust belt, northwestern Argentina. *Tectonics*, *21*(6), 11-1–11-18.

Kley, J., Monaldi, C. R., & Salfity, J. A. (1999). Along-strike segmentation of the Andean foreland: Causes and consequences. *Tectonophysics*, *301*(1–2), 75–94. https://doi.org/10.1016/s0040-1951(98)90223-2

Kley, J., Rossello, E. A., Monaldi, C. R., & Habighorst, B. (2005). Seismic and field evidence for selective inversion of Cretaceous normal faults, Salta rift, northwest Argentina. *Tectonophysics*, *399*(1–4), 155–172. (SPEC. ISS.). https://doi.org/10.1016/j.tecto.2004.12.020

Kostrov, B. V. (1974). Seismic moment and energy of earthquakes, and seismic flow of rock. *Physics of the Solid Earth*, *1*, 13–21.

Lamb, S. (2006). Shear stresses on megathrusts: Implications for mountain building behind subduction zones. *Journal of Geophysical Research: Solid Earth*, *111*(B7), B07401. https://doi.org/10.1029/2005jb003916

Lamb, S. H. (2000). Active deformation in the Bolivian Andes, south America. *Journal of Geophysical Research: Solid Earth*, *105*(B11), 25627–25653. https://doi.org/10.1029/2000jb900187

Legrand, D., Baby, P., Bondoux, F., Dorbath, C., Bès de Berc, S., & Rivadeneira, M. (2005). The 1999-2000 seismic experiment of Macas swarm (Ecuador) in relation with rift inversion in Subandean foothills. *Tectonophysics*, *395*(1–2), 67–80. https://doi.org/10.1016/j.tecto.2004.09.008

Lucassen, F., Franz, G., Viramonte, J., Romer, R. L., Dulski, P., & Lang, A. (2005). The late Cretaceous lithospheric mantle beneath the Central Andes: Evidence from phase equilibria and composition of mantle xenoliths. *Lithos*, *82*(3–4), 379–406. https://doi.org/10.1016/j.lithos.2004.08.002

Lucassen, F., Lewerenz, S., Franz, G., Viramonte, J., & Mezger, K. (1999). Metamorphism, isotopic ages and composition of lower crustal granulite xenoliths from the Cretaceous Salta Rift, Argentina. *Contributions to Mineralogy and Petrology*, *134*(4), 325–341. https://doi.org/10.1007/s004100050488

Lund, M. G., Austrheim, H., & Erambert, M. (2004). Earthquakes in the deep continental crust-insights from studies on exhumed high-pressure rocks. *Geophysical Journal International*, *158*(2), 569–576. https://doi.org/10.1111/j.1365-246x.2004.02368.x

Lyon-Caen, H., Molnar, P., & Suárez, G. (1985). Gravity anomalies and flexure of the Brazilian shield beneath the Bolivian Andes. *Earth and Planetary Science Letters*, *75*(1), 81–92. https://doi.org/10.1016/0012-821x(85)90053-6

Mackwell, S. J., Zimmerman, M. E., & Kohlstedt, D. L. (1998). High-temperature deformation of dry diabase with application to tectonics on Venus. *Journal of Geophysical Research: Solid Earth*, *103*(1), 975–984. https://doi.org/10.1029/97jb02671

Maggi, A., Jackson, J. A., McKenzie, D., & Priestley, K. (2000). Earthquake focal depths, effective elastic thickness, and the strength of the continental lithosphere. *Geology*, *28*(6), 495–498. https://doi.org/10.1130/0091-7613(2000)028<0495:efdeet>2.3.co;2

Maggi, A., Jackson, J. A., Priestley, K., & Baker, C. (2000). A re-assessment of focal depth distributions in southern Iran, the tien Shan and northern India: Do earthquakes really occur in the continental mantle? *Geophysical Journal International*, *143*(3), 629–661. https://doi.org/10.1046/j.1365-246x.2000.00254.x

Mathalone, J. M. P., & Montoya, M. R. (1995). Petroleum geology of the sub-andean basins of Peru. In *Petroleum basins of South America* (pp. 423–444). AAPG Special Volumes.

McGroder, M. F., Lease, R. O., & Pearson, D. M. (2015). Along-strike variation in structural styles and hydrocarbon occurrences, Subandean fold-and-thrust belt and inner foreland, Colombia to Argentina. In P. G. DeCelles, M. N. Ducea, B. Carrapa, & P. A. Kapp (Eds.), *Geodynamics of a cordilleran orogenic system: The central Andes of Argentina and northern Chile*. Geological Society of America.

McKenzie, D., Jackson, J., & Priestley, K. (2005). Thermal structure of oceanic and continental lithosphere. *Earth and Planetary Science Letters*, *233*(3), 337–349. https://doi.org/10.1016/j.epsl.2005.02.005

McKenzie, D., & Priestley, K. (2016). Speculations on the formation of cratons and cratonic basins. *Earth and Planetary Science Letters*, *435*, 94–104. https://doi.org/10.1016/j.epsl.2015.12.010

Meigs, A. J., & Nabelek, J. (2010). Crustal-scale pure shear foreland deformation of Western Argentina. *Geophysical Research Letters*, *37*(11). https://doi.org/10.1029/2010gl043220

Menegon, L., Pennacchioni, G., Malaspina, N., Harris, K., & Wood, E. (2017). Earthquakes as precursors of ductile shear zones in the dry and strong lower crust. *Geochemistry, Geophysics, Geosystems*, *18*(12), 4356–4374. https://doi.org/10.1002/2017gc007189

Mercier, J. L., Sebrier, M., Lavenu, A., Cabrera, J., Bellier, O., Dumont, J.-F., & Machrare, J. (1992). Changes in the tectonic regime above a subduction zone of andean type: The Andes of Peru and Bolivia during the pliocene-pleistocene. *Journal of Geophysical Research*, *97*(B8), 11945. https://doi.org/10.1029/90jb02473

Molnar, P., Chen, W.-P., Fitch, T. J., Tapponnier, P., Warsi, W. E. K., & Wu, F. (1977). Structure and tectonics of the himalaya: A brief summary of relevant geophysical observations. In *Collogue Internationaux du CNRS, No. 268, Himalaya: Sciences de la Terre* (pp. 269–294). du Centre National de la Recherche Scientifique.

Molnar, P., & Lyon-Caen, H. (1988). Some simple physical aspects of the support, structure, and evolution of mountain belts. *Geological Society of America Special Paper*. Geological Society of America. (Vol. *218*, pp. 179–208).

Molnar, P., & Lyon-Caen, H. (1989). Fault plane solutions of earthquakes and active tectonics of the Tibetan Plateau and its margins. *Geophysical Journal International*, *99*(1), 123–154. https://doi.org/10.1111/j.1365-246x.1989.tb02020.x

Mora, A., Parra, M., Strecker, M. R., Kammer, A., Dimaté, C., & Rodríguez, F. (2006). Cenozoic contractional reactivation of Mesozoic extensional structures in the Eastern Cordillera of Colombia. *Tectonics*, *25*(2). https://doi.org/10.1029/2005tc001854

Newton, R. C. (1990). Fluids and shear zones in the deep crust. *Tectonophysics*, *182*(1–2), 21–37. https://doi.org/10.1016/0040-1951(90)90339-a

Nocquet, J. M., Villegas-Lanza, J. C., Chlieh, M., Mothes, P. A., Rolandone, F., Jarrin, P., et al. (2014). Motion of continental slivers and creeping subduction in the northern Andes. *Nature Geoscience*, *7*(4), 287–291. https://doi.org/10.1038/ngeo2099

Oncken, O., Boutelier, D., Dresen, G., & Schemmann, K. (2012). Strain accumulation controls failure of a plate boundary zone: Linking deformation of the Central Andes and lithosphere mechanics. *Geochemistry, Geophysics, Geosystems*, *13*(12). https://doi.org/10.1029/2012gc004280

Oncken, O., Hindle, D., Kley, J., Elger, K., Victor, P., & Schemmann, K. (2006). Deformation of the central andean upper plate system Äî facts, fiction, and constraints for plateau models. In *The Andes* (pp. 3–27). Springer Berlin Heidelberg.

Poveda, E., Monsalve, G., & Vargas, C. A. (2015). Receiver functions and crustal structure of the northwestern Andean region, Colombia. *Journal of Geophysical Research: Solid Earth*, *120*(4), 2408–2425. https://doi.org/10.1002/2014jb011304

Priestley, K., & McKenzie, D. (2013). The relationship between shear wave velocity, temperature, attenuation and viscosity in the shallow part of the mantle. *Earth and Planetary Science Letters*, *381*, 78–91. https://doi.org/10.1016/j.epsl.2013.08.022

Ramos, V. A. (2009). Anatomy and global context of the Andes: Main geologic features and the Andean orogenic cycle. In S. M. Kay, V. A. Ramos, & W. R. Dickinson (Eds.), *Backbone of the americas: Shallow subduction, plateau uplift ad terrane collision* (pp. 31–65). Geological Society of America Memoir.

Ramos, V. A. (2010a). The grenville-age basement of the Andes. *Journal of South American Earth Sciences*, *29*(1), 77–91. https://doi.org/10.1016/j.jsames.2009.09.004

Ramos, V. A. (2010b). The tectonic regime along the Andes: Present-day and Mesozoic regimes. *Geological Journal*, *45*(1), 2–25. https://doi.org/10.1002/gj.1193

Ramos, V. A., Cristallini, E. O., & Pérez, D. J. (2002). The pampean flat-slab of the central Andes. *Journal of South American Earth Sciences*, *15*(1), 59–78. https://doi.org/10.1016/s0895-9811(02)00006-8

Rapela, C. W., Pankhurst, R. J., Casquet, C., Baldo, E., Galindo, C., Fanning, C. M., & Dahlquist, J. M. (2010). The Western Sierras Pampeanas: Protracted Grenville-age history (1330-1030 Ma) of intra-oceanic arcs, subduction-accretion at continental-edge and AMCG intraplate magmatism. *Journal of South American Earth Sciences*, *29*(1), 105–127. https://doi.org/10.1016/j.jsames.2009.08.004

Rapela, C. W., Pankhurst, R. J., Casquet, C., Baldo, E., Saavedra, J., Galindo, C., & Fanning, C. M. (1998). The Pampean Orogeny of the southern proto-Andes: Cambrian continental collision in the Sierras de Cordoba. *Geological Society - Special Publications*, *142*(i), 181–217. https://doi.org/10.1144/gsl.sp.1998.142.01.10

Richardson, R. M., & Coblentz, D. D. (1994). Stress modeling in the Andes: Constraints on the South American intraplate stress magnitudes. *Journal of Geophysical Research: Solid Earth*, *99*(B11), 22015–22025. https://doi.org/10.1029/94jb01751

Richardson, T., Gilbert, H., Anderson, M., & Ridgway, K. D. (2012). Seismicity within the actively deforming eastern sierras Pampeanas, Argentina. *Geophysical Journal International*, *188*(2), 408–420. https://doi.org/10.1111/j.1365-246x.2011.05283.x

Rivas, C., Ortiz, G., Alvarado, P., Podesta, M., & Martin, A. (2019). Modern crustal seismicity in the northern Andean Precordillera, Argentina. *Tectonophysics*, *762*(January), 144–158. https://doi.org/10.1016/j.tecto.2019.04.019

Rybacki, E., & Dresen, G. (2004). Deformation mechanism maps for feldspar rocks. *Tectonophysics*, *382*(3–4), 173–187. https://doi.org/10.1016/j.tecto.2004.01.006

Salfity, J. A., & Marquillas, R. A. (1994). Tectonic and sedimentary evolution of the cretaceous-eocene Salta group basin, Argentina. In J. A. Salfity (Ed.), *Cretaceous tectonics of the Andes* (pp. 266–315). Vieweg.

Sandiford, M., & Powell, R. (1986). Deep crustal metamorphism during continental extension: Modern and ancient examples. *Earth and Planetary Science Letters*, *79*(1–2), 151–158. https://doi.org/10.1016/0012-821x(86)90048-8

Sempere, T., Carlier, G., Soler, P., Fornari, M., Carlotto, V., Jacay, J., et al. (2002). Late Permian-Middle Jurassic lithospheric thinning in Peru and Bolivia, and its bearing on Andean-age tectonics. *Tectonophysics*, *345*(1–4), 153–181. https://doi.org/10.1016/s0040-1951(01)00211-6

Sibson, R. H. (1982). Fault zone models, heat flow, and the depth distribution of earthquakes in the continental crust of the United States. *Bulletin of the Seismological Society of America*, *72*(1), 151–163.

Sibson, R. H. (1990). Conditions for fault-valve behaviour. *Geological Society - Special Publications*, *54*(1), 15–28. https://doi.org/10.1144/gsl.sp.1990.054.01.02

Sibson, R. H. (1995). Selective fault reactivation during basin inversion: Potential for fluid redistribution through fault-valve action. *Geological Society - Special Publications*, *88*(88), 3–19. https://doi.org/10.1144/gsl.sp.1995.088.01.02

Sloan, R. A., Jackson, J. A., McKenzie, D., & Priestley, K. (2011). Earthquake depth distributions in central Asia, and their relations with lithosphere thickness, shortening and extension. *Geophysical Journal International*, *185*(1), 1–29. https://doi.org/10.1111/j.1365-246x.2010.04882.x

Smalley, R., & Isacks, B. L. (1990). Seismotectonics of thin- and thick-skinned deformation in the andean foreland from local network data: Evidence for a seismogenic lower crust. *Journal of Geophysical Research*, *95*(B8), 12487–12498. https://doi.org/10.1029/jb095ib08p12487

Smalley, R., Pujol, J., Regnier, M., Chiu, J. M., Chatelain, J. L., Isacks, B. L., et al. (1993). Basement seismicity beneath the Andean precordillera thin̂ĉskinned thrust belt and implications for crustal and lithospheric behavior. *Tectonics*, *12*(1), 63–76. https://doi.org/10.1029/92tc01108

Sobolev, S., & Babeyko, A. (2005). What drives orogeny in the Andes? *Geology*, *33*(8), 617–620. https://doi.org/10.1130/g21557ar.1

Sørensen, B. E., Grant, T., Ryan, E. J., & Larsen, R. B. (2019). In situ evidence of earthquakes near the crust mantle boundary initiated by mantle CO2 fluxing and reaction-driven strain softening. *Earth and Planetary Science Letters*, *524*, 115713. https://doi.org/10.1016/j.epsl.2019.115713

Sørensen, K. (1983). Growth and dynamics of the Nordre Stromfjord shear zone. *Journal of Geophysical Research*, *88*(B4), 3419–3437. https://doi.org/10.1029/jb088ib04p03419

Spikings, R., Reitsma, M. J., Boekhout, F., Mišković, A., Ulianov, A., Chiaradia, M., et al. (2016). Characterisation of Triassic rifting in Peru and implications for the early disassembly of Western Pangaea. *Gondwana Research*, *35*, 124–143. https://doi.org/10.1016/j.gr.2016.02.008

Starck, D. (2010). Cuenca cretàcica-paleógena del Noroeste argentino. In *VIII congreso de Exploración y desarrollo de Hidrocarburos simposio cuencas argentinas* (pp. 407–453). Instituto Argentino del Petróleo y el Gas.

Stewart, J., & Watts, A. B. (1997). Gravity anomalies and spatial variations of flexural rigidity at mountain ranges. *Journal of Geophysical Research: Solid Earth*, *102*(B3), 5327–5352. https://doi.org/10.1029/96jb03664

Suárez, G., Gagnepain, J., Cisternas, A., Hatzfeld, D., Molnar, P., Ocola, L., et al. (1990). Tectonic deformation of the Andes and the configuration of the subducted slab in central Peru; results from a microseismic experiment. *Geophysical Journal International*, *103*(1), 1–12. https://doi.org/10.1111/j.1365-246x.1990.tb01747.x

Suarez, G., Molnar, P., & Burchfiel, B. C. (1983). Seismicity, fault plane solutions, depth of faulting, and active tectonics of the Andes of Peru, Ecuador, and southern Colombia. *Journal of Geophysical Research*, *88*(B12), 10403–10428. https://doi.org/10.1029/jb088ib12p10403

Taymaz, T., Jackson, J. A., & Westaway, R. (1990). Earthquake mechanisms in the hellenic trench near crete. *Geophysical Journal International*, *102*(3), 695–731. https://doi.org/10.1111/j.1365-246x.1990.tb04590.x

Turcotte, D. L., & Schubert, G. (2002). *Geodynamics*. Cambridge University Press.

Vaca, S., Vallée, M., Nocquet, J. M., & Alvarado, A. (2019). Active deformation in Ecuador enlightened by a new waveform-based catalog of earthquake focal mechanisms. *Journal of South American Earth Sciences*, *93*, 449–461. https://doi.org/10.1016/j.jsames.2019.05.017

Watts, A., Lamb, S., Fairhead, J., & Dewey, J. (1995). Lithospheric flexure and bending of the central Andes. *Earth and Planetary Science Letters*, *134*(1–2), 9–21. https://doi.org/10.1016/0012-821x(95)00095-t

Weiss, J. R., Brooks, B. A., Arrowsmith, J. R., & Vergani, G. (2015). Spatial and temporal distribution of deformation at the front of the Andean orogenic wedge in southern Bolivia. *Journal of Geophysical Research: Solid Earth*, *120*(3), 1909–1931. https://doi.org/10.1002/2014jb011763

Weller, O. M., Mottram, C. M., St-Onge, M. R., Möller, C., Strachan, R., Rivers, T., & Copley, A. (2021). *The metamorphic and magmatic record of collisional orogens* (pp. 1–19). Nature Reviews Earth & Environment.

Whyte, A. J., Weller, O. M., Copley, A. C., & St-Onge, M. R. (2021). Quantifying water diffusivity and metamorphic reaction rates within mountain belts, and their implications for the rheology of cratons. *Geochemistry, Geophysics, Geosystems*. https://doi.org/10.1029/2021gc00998

Wimpenny, S., Benavente, C., Copley, A., Garcia, B., Rossell, L., O'Kane, A., & Aguirre, E. (2020). Observations and dynamical implications of active normal faulting in south Peru. *Geophysical Journal International*, *222*(1), 27–53. https://doi.org/10.1093/gji/ggaa144

Wimpenny, S., Copley, A., Benavente Escobar, C. L., & Aguirre, E. (2018). Extension and dynamics of the Andes inferred from the 2016 parina (huarichancara) earthquake. *Journal of Geophysical Research: Solid Earth*, *123*(9), 8198–8228. https://doi.org/10.1029/2018jb015588

Yardley, B. W. D., & Valley, J. W. (1997). The petrologic case for a dry lower crust. *Journal of Geophysical Research*, *102*(97), 12173–12185. https://doi.org/10.1029/97jb00508

Zwick, P., McCaffrey, R., & Abers, G. (1994). MT5 Program.